

Genetically-targeted photorelease of endocannabinoids enables optical control of GPR55 in pancreatic β -cells

Janelle M. Tobias^{1,2,3}, Gabriela Rajic¹, Alexander E.G. Viray^{1,2}, David Icka-Araki^{1,2,4}
and James A. Frank^{*1,2}

¹Vollum Institute, Oregon Health & Science University, Portland, OR, USA

²Department of Chemical Physiology & Biochemistry, Oregon Health & Science University, Portland, OR, USA.

³Graduate Program in Physiology & Pharmacology, Oregon Health & Science University, Portland, OR, USA

⁴Graduate Program in Biomedical Sciences, Oregon Health & Science University, Portland, OR, USA

*correspondence: frankja@ohsu.edu

SUPPLEMENTARY INFORMATION

SUPPLEMENTARY FIGURES

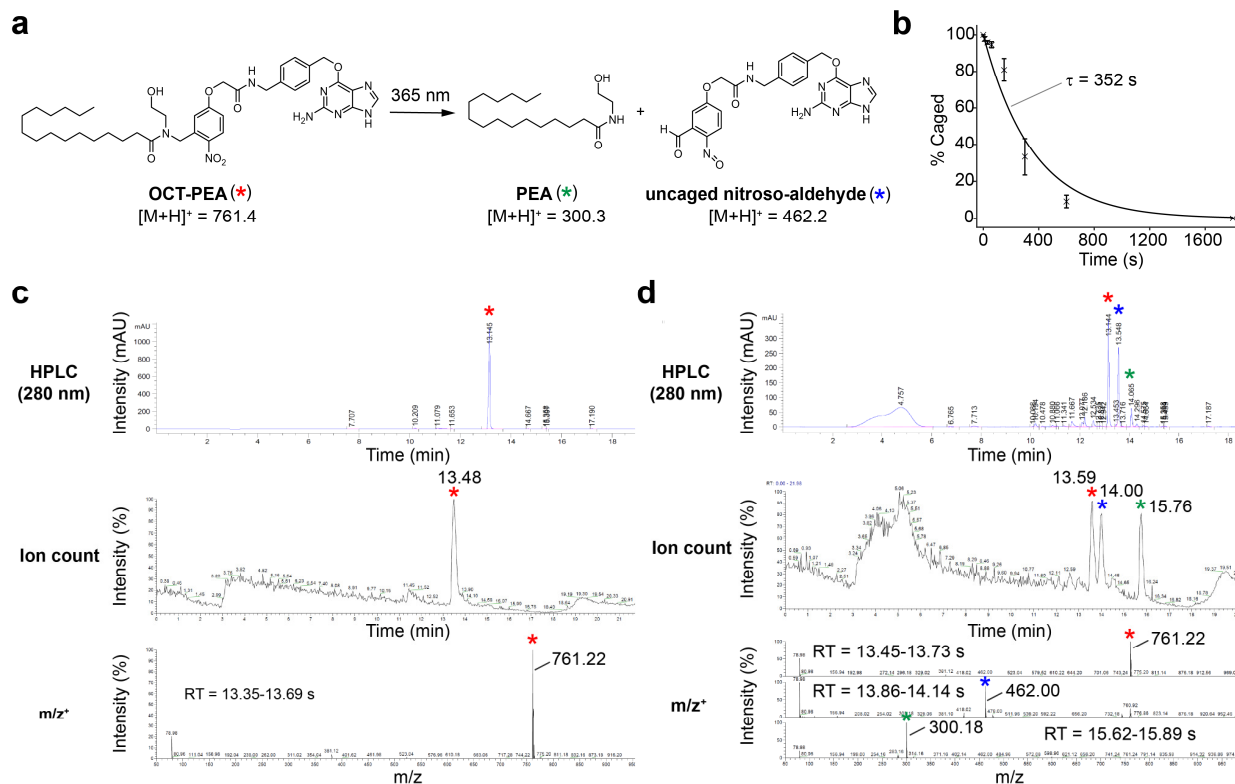


Figure S1. HPLC-MS characterization of OCT-PEA uncaging in DMSO. (a) Chemical structures showing the uncaging reaction of OCT-PEA, alongside predicted $[M+H]^+$ for the main species. (b) Uncaging curve of OCT-PEA (5 mM in DMSO, N = 4) determined by HPLC. Error bars = mean \pm S.E.M (c,d) HPLC-MS analysis of OCT-PEA both (c) before uncaging, and (d) after uncaging with 365 nm light for 10 min. Shown are (top) the HPLC absorption intensity at 280 nm over time, (middle) ion count over time, and (bottom) m/z^+ profile for the specified retention time (RT). Masses for the main peaks are accentuated, and each species is marked by a colored star. Red = OCT-PEA, blue = uncaged nitroso-aldehyde, and green = PEA.

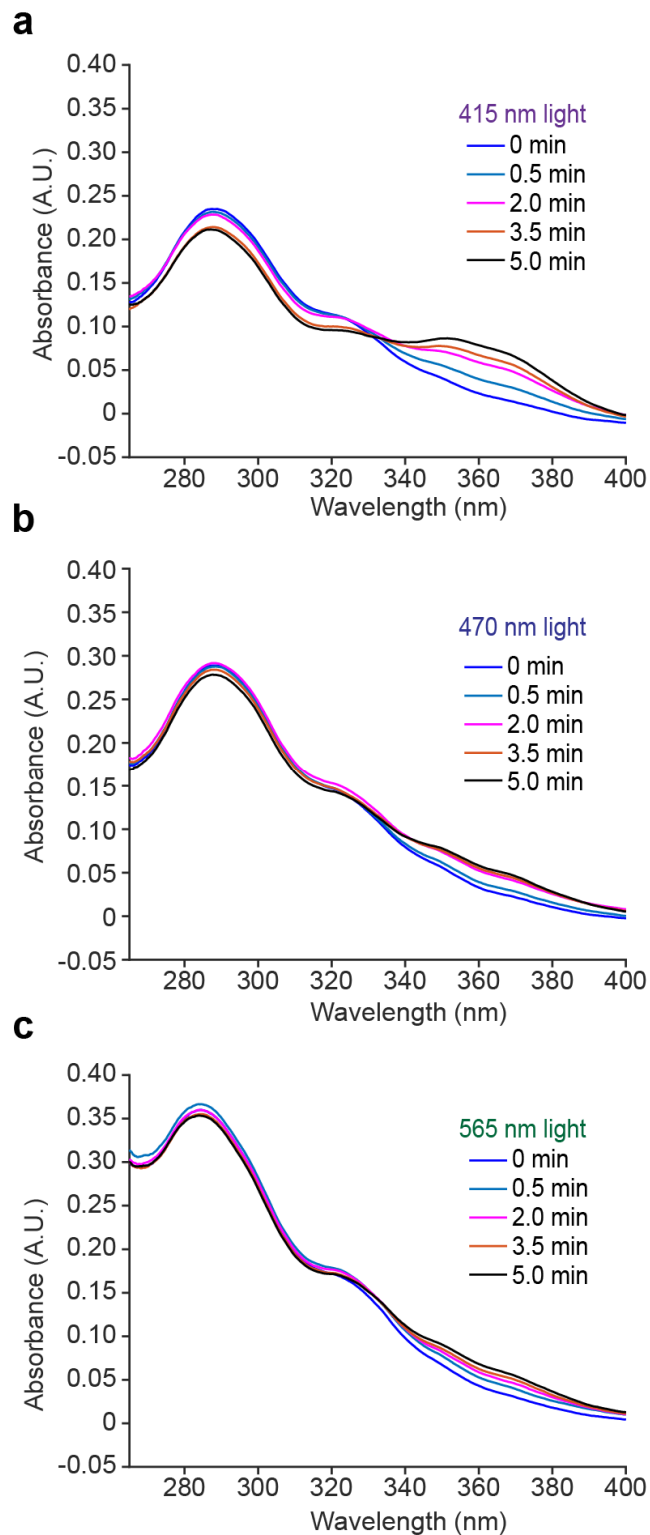


Figure S2. UV-Vis characterization of OCT-PEA. Absorbance vs. wavelength scan of OCT-PEA (20 μM, in DMSO) after uncaging using (a) 415 nm (b) 470 nm (c) 565 nm LEDs for 5 min.

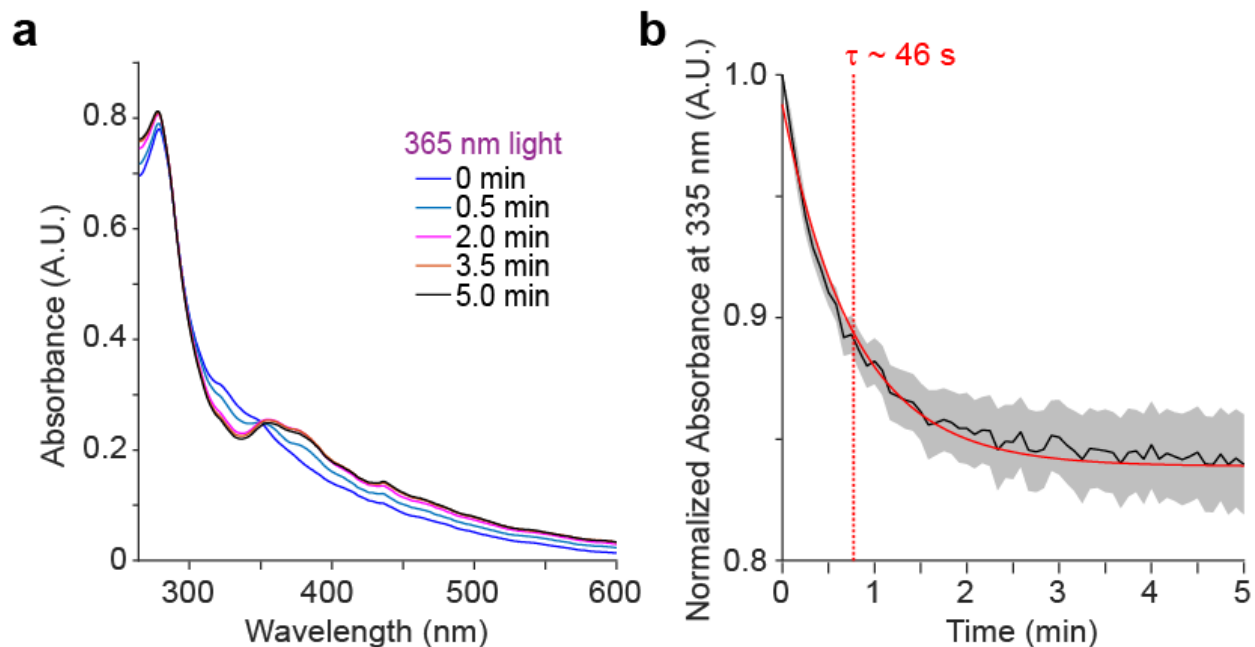


Figure S3. UV-Vis characterization of SNAP-tag-tethered OCT-PEA. (a) Absorbance vs wavelength of scan of OCT-PEA after it had been conjugated to purified SNAP-tag in the presence of SNAP-tag purified protein (10 μ M in PBS). (b) Absorbance over time at $\lambda = 335$ nm of OCT-PEA in the presence of SNAP-tag purified protein. Red dotted line indicates $\tau \sim 46$ s for OCT-PEA uncaging under 365 nm LED irradiation. The exponential best-fit is displayed as a solid red line. N = 3 trials. Shaded error bars = mean \pm S.E.M.

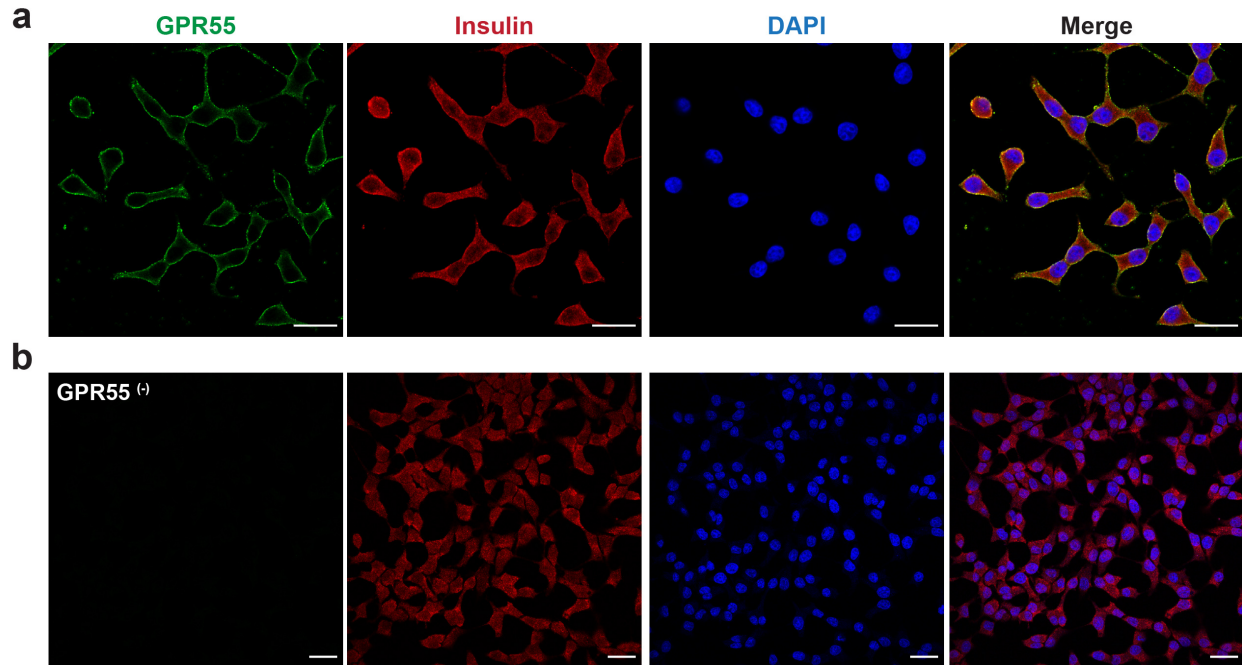


Figure S4. INS-1 β -cells express GPR55 and insulin. Double immunofluorescence staining of GPR55 (green) and insulin (red). DAPI (blue) was used as a nuclear marker. Displayed are individual channels and the merged image. **(a)** Zoomed out images of cells shown in Figure 3A. **(b)** Control experiment without the GPR55 primary antibody. No GPR55 immunofluorescence is observed, demonstrating that the effect is not caused by non-specific secondary antibody binding. Scale bars = 20 μ m.

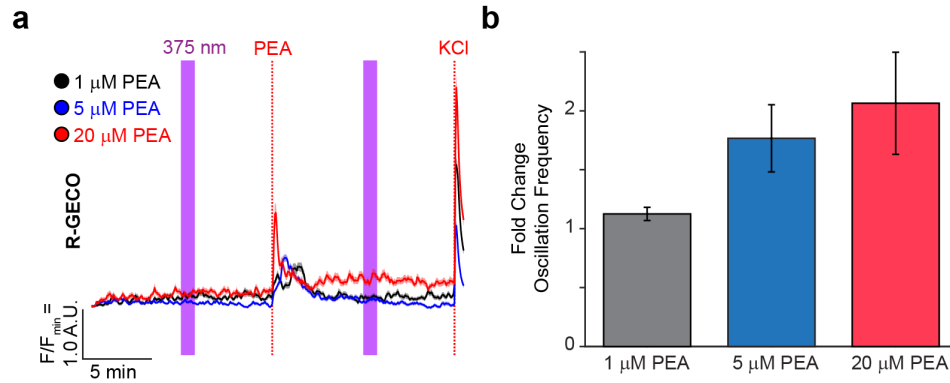


Figure S5. PEA stimulates β -cell Ca^{2+} in a concentration-dependent manner. (a) Average $[\text{Ca}^{2+}]_i$ traces for R-GECO-transfected INS-1 cells in response to 1 μM PEA (black, N = 165, T = 3), 5 μM PEA (blue, N = 494, T = 7), and 20 μM PEA (red, N = 224, T = 4). (b) Bar graph displaying the fold change in Ca^{2+} oscillation frequency after PEA addition relative to baseline (before PEA addition).

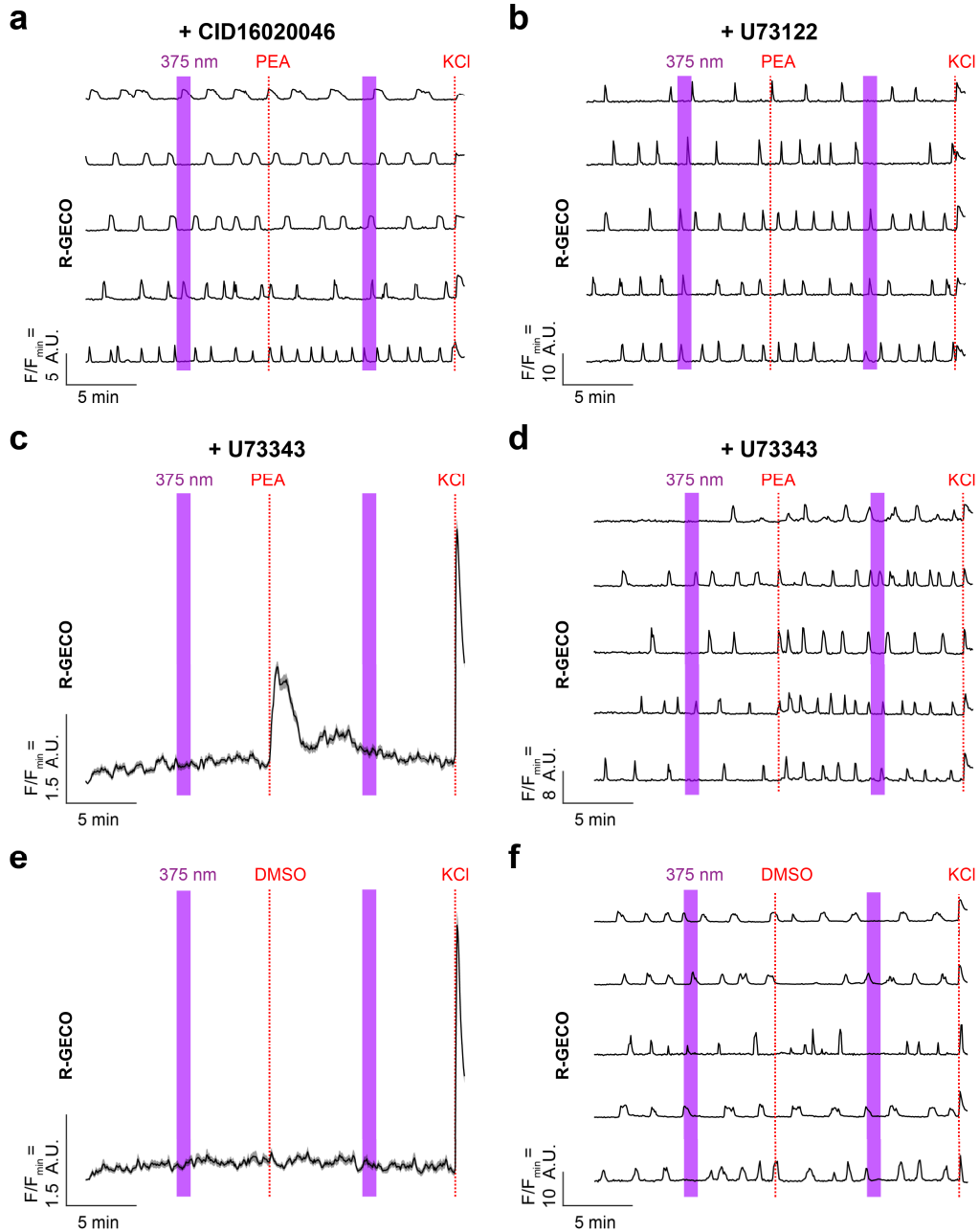


Figure S6. INS-1 Ca^{2+} imaging controls for PEA addition. Fluorescent Ca^{2+} imaging with R-GECO in INS-1 cells showed that pre-incubation with (a) CID16020046 ($5 \mu\text{M}$, $N = 449$, $T = 6$) and (b) U73122 ($5 \mu\text{M}$, $N = 296$, $T = 4$) blocked the effect of PEA ($5 \mu\text{M}$), displayed as representative traces from five cells. (c,d) Pre-incubation with U73343 ($5 \mu\text{M}$, $N = 511$, $T = 7$) did not block the effect the Ca^{2+} response induced by PEA, displayed as (c) the average and (d) representative traces from five cells. (e,f) INS-1 cells did not respond to 365 nm irradiation (shaded purple bars), nor a vehicle addition (0.1 vol% DMSO, $N = 418$, $T = 6$), displayed as (e) the average and (f) traces from five representative cells. Error bars = mean \pm S.E.M.

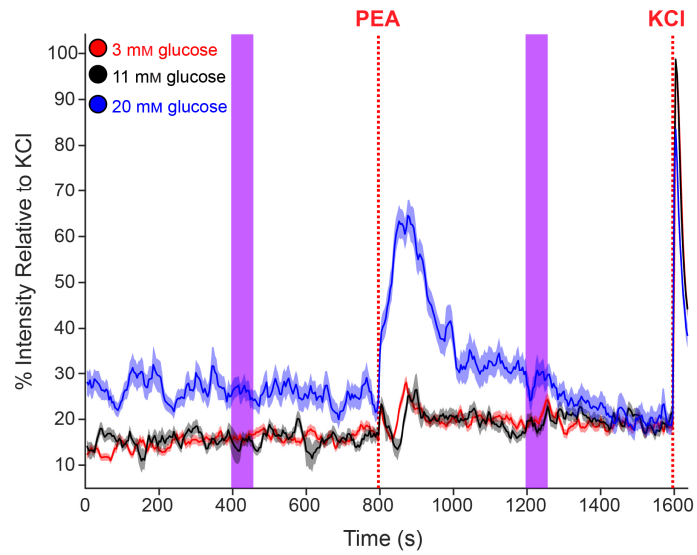


Figure S7. PEA stimulates Ca^{2+} in a glucose concentration-dependent manner.

Fluorescent Ca^{2+} imaging with R-GECO in INS-1 cells showed that PEA addition caused an increase in Ca^{2+} in a glucose-dependent manner. Shown is the response to a $5 \mu\text{M}$ PEA addition at a glucose concentration of 20 mM (blue, N = 494, T = 7), 11 mM (black, N = 307, T = 4) and 3 mM (red, N = 485, T = 6). Shaded error bars = mean \pm S.E.M.

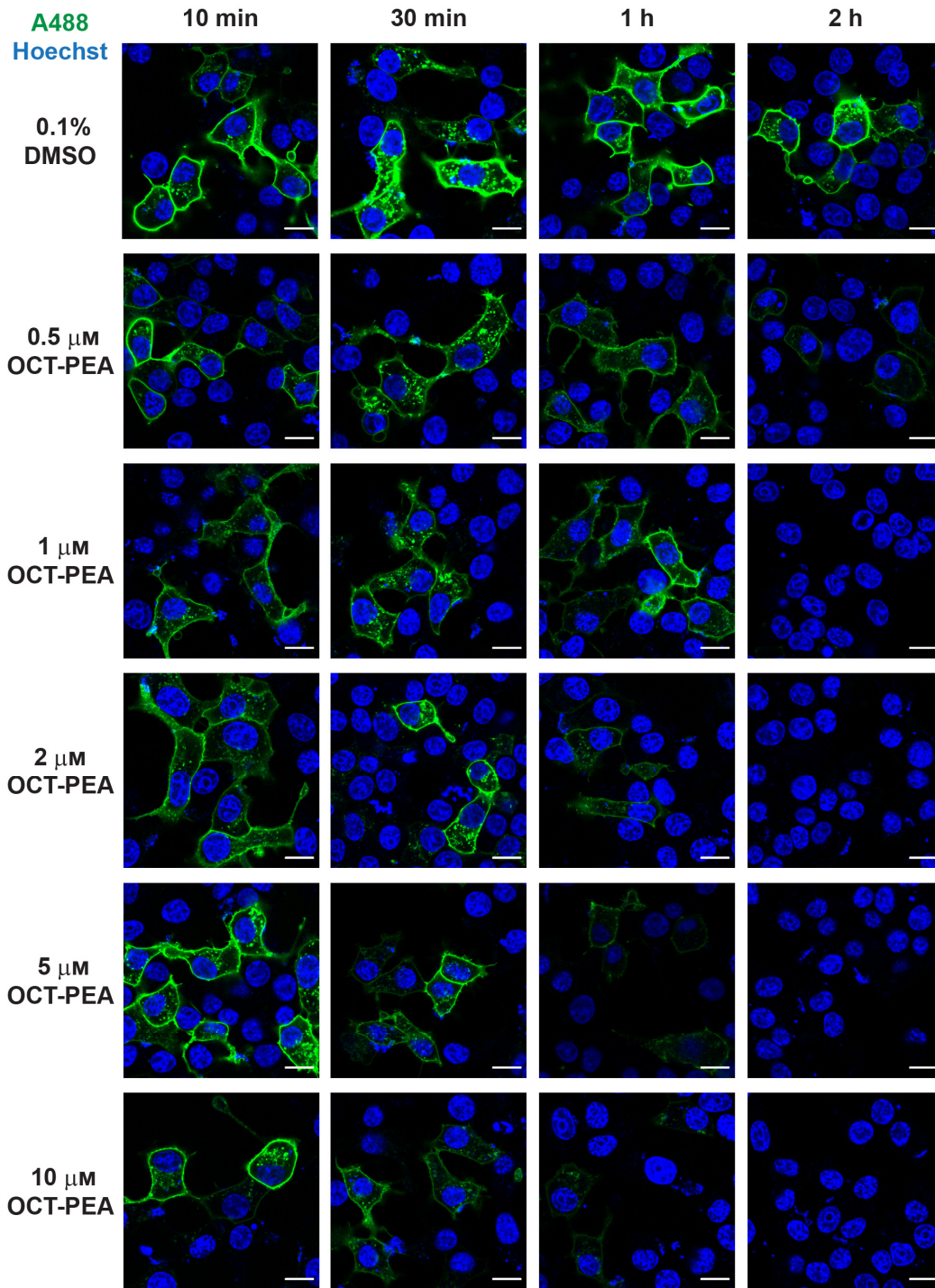


Figure S8. OCT-PEA labelling optimization. OCT-PEA labels SNAP-tags in a time and concentration dependent manner. INS-1 cells transfected with pDisplayTM-SNAP were treated with probe first, washed, then stained with SNAP-Surface[®] Alexa Fluor[®] 488 (A488, green). SNAP-tags that were not completely labeled with OCT-PEA are thus shown in green. Hoechst-33342 (blue) was used as a nuclear marker. Scale bars = 10 μm.

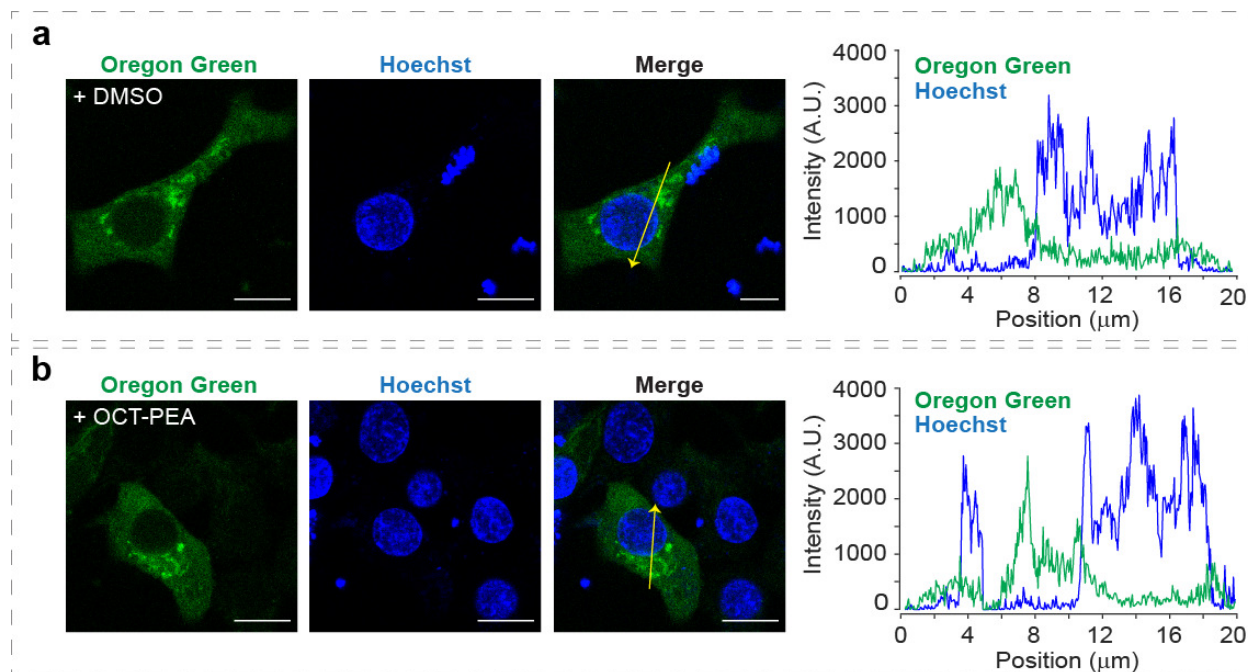


Figure S9. SNAP-Cell® Oregon Green® labelling. INS-1 cells transfected with pDisplay™-SNAP were treated with DMSO (0.1% v/v, **a**) or OCT-PEA (5 µM, **b**) for 2 h, followed by incubation with cell-permeable SNAP-Cell® Oregon Green® (1 µM, 30 min). Hoechst-33342 (blue) serves as a nuclear marker. Intensity values of green and blue channels plotted along the yellow line shown in the merge image. Scale bars = 10 µm.

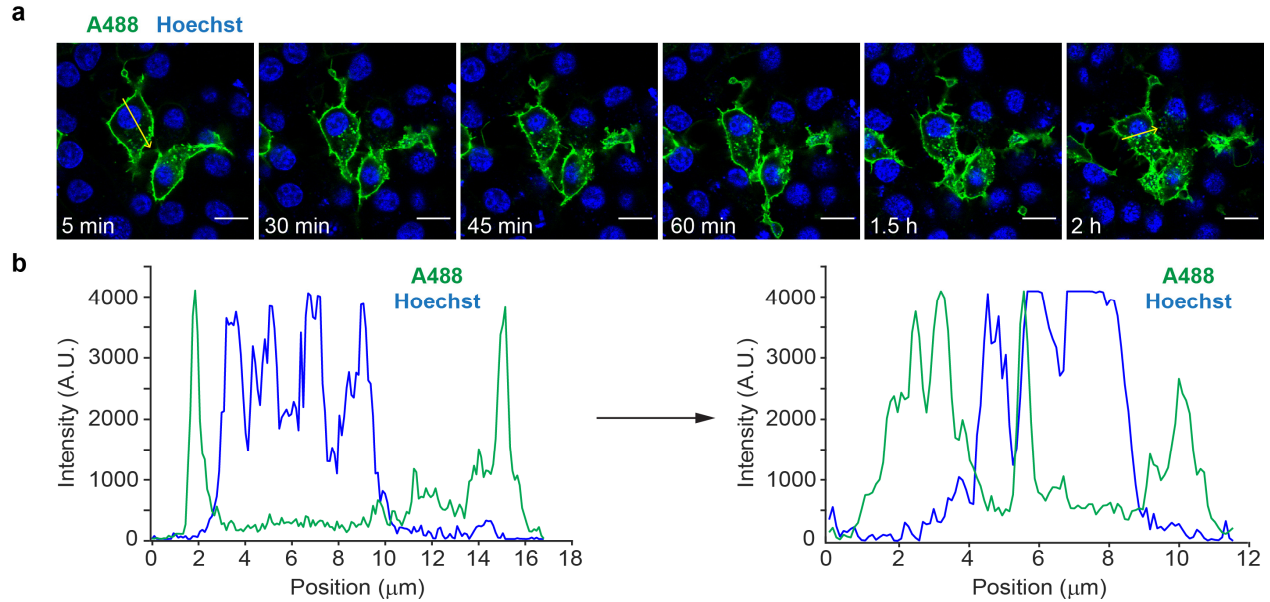


Figure S10. SNAP-tag internalization after prolonged labeling. (a) INS-1 cells transfected with pDisplayTM-SNAP were labeled with non-permeably dye SNAP-Surface[®] Alexa Fluor[®] 488 (A488, 1 μ M, 30 min, green), washed, and imaged over time. Hoechst-33342 (blue) serves as a nuclear marker. Displayed are representative images of the same cells over time. (b) Intensity values of green and blue channels along the yellow line shown in (a), at 5 min (left) and 2 h (right) post wash. While some SNAP-tags are internalized over time, a majority remains enriched at the plasma membrane. Scale bars = 10 μ m.

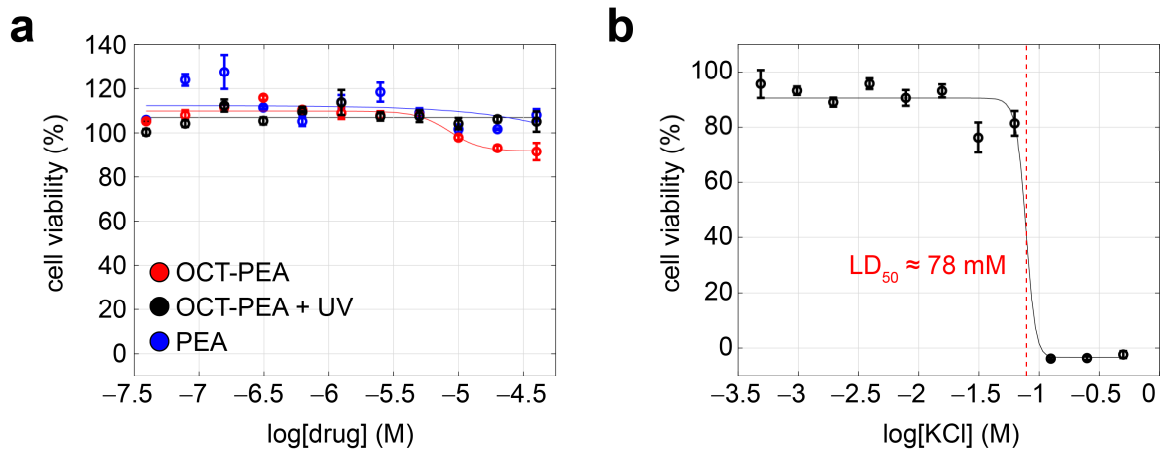


Figure S11. Cell viability assay. INS-1 cells were incubated with compound for 24 h, then evaluated by the 3-(4,5-dimethylthiazol-2-yl)-2,5-diphenyltetrazolium bromide (MTT) assay. **(a)** INS-1 cell viability remained stable when the cells were incubated with OCT-PEA (caged, red), UV-A irradiated OCT-PEA (uncaged, black) or PEA (blue) up to 40 μ M, near its solubility limit in physiological buffer. **(b)** As a positive control for the assay, INS-1 cells were incubated with KCl for 24 h, which had an LD_{50} of \sim 78 mM. Four biological replicates were performed for each condition. Error bars = mean \pm S.E.M.

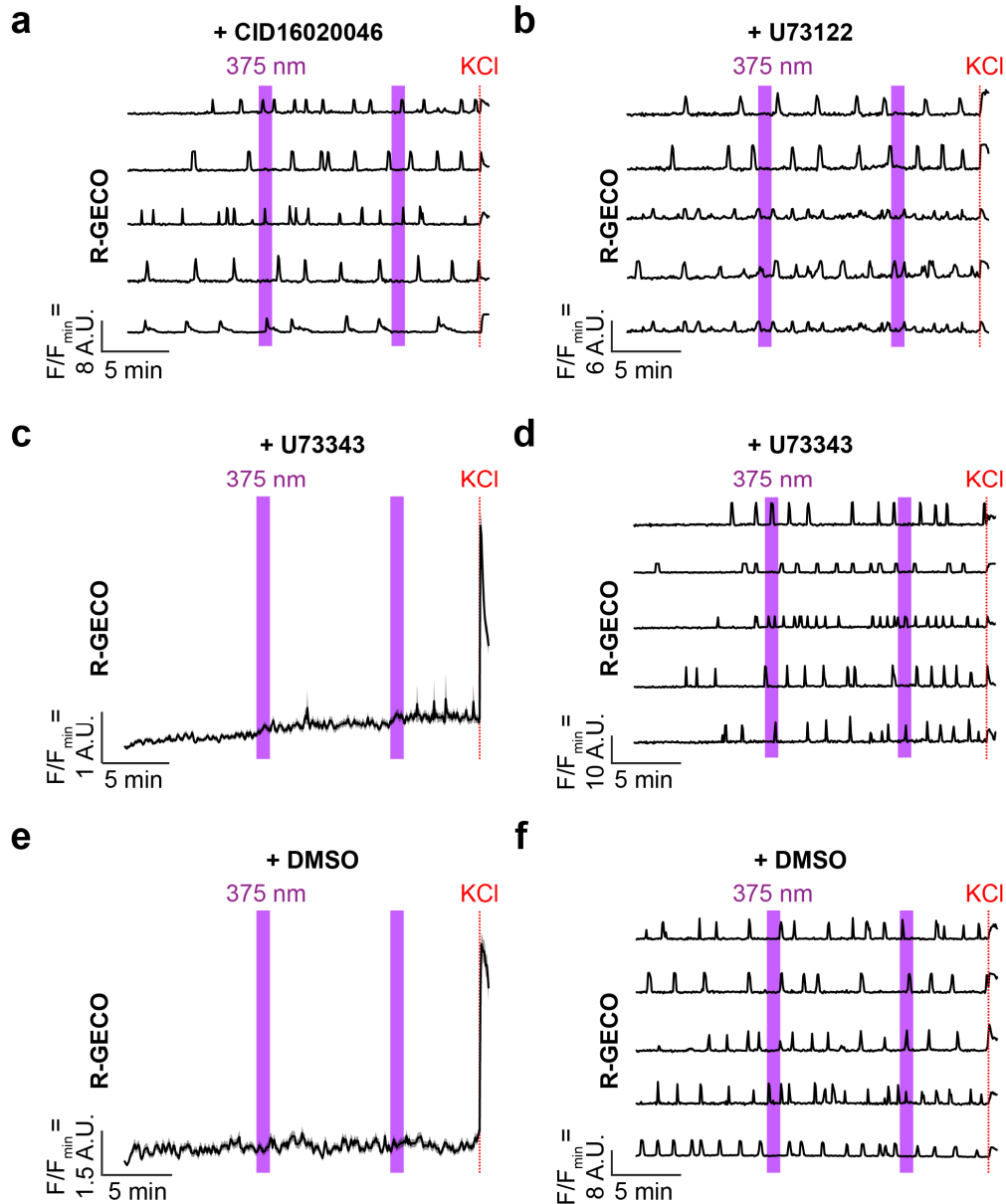


Figure S12. Ca^{2+} imaging controls for OCT-PEA uncaging in INS-1 cells. Fluorescent Ca^{2+} imaging in INS-1 cells expressing R-GECO and pDisplayTM-SNAP revealed that OCT-PEA (5 μ M, 2 h) uncaging activates GPR55 through PLC. (a,b) Pre-incubation with (a) CID16020046 (5 μ M, 30 min, N = 212, T = 4) and (b) U73122 (5 μ M, 30 min, N = 173, T = 4) abolished the effect of OCT-PEA uncaging; displayed as representative traces from five cells. (c,d) Pre-incubation with U73343 (5 μ M, 30 min, N = 357, T = 6) did not block the effect of OCT-PEA, displayed as (c) average and (d) representative traces from five cells. (e, f) Pre-incubation with vehicle (0.1% v/v DMSO, 2 h, N = 247, T = 4) did not sensitize the cells to UV-irradiation; displayed as (e) average and (f) representative traces from five cells. Shaded error bars = mean \pm S.E.M.

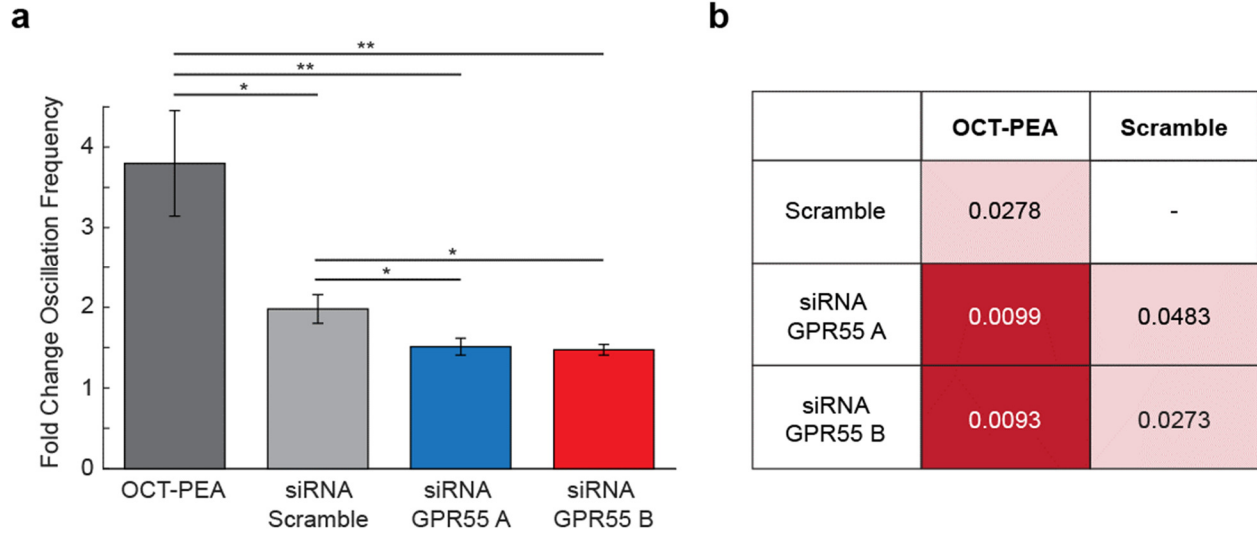


Figure S13. Ca²⁺ imaging for OCT-PEA uncaging in siRNA knockdown INS-1 cells. Fluorescent Ca²⁺ imaging in INS-1 cells transfected with siRNA scramble (N = 300, T = 8), siRNA GPR55 A (N = 160, T = 4), or siRNA GPR55 B (N = 177, T = 4), and expressing R-GECO and pDisplayTM-SNAP. Standard conditions without siRNA transfection (OCT-PEA, N = 398, T = 8) shown for comparison. Error bars = mean ± S.E.M. **P<0.01 (dark red), *P<0.05 (pink).

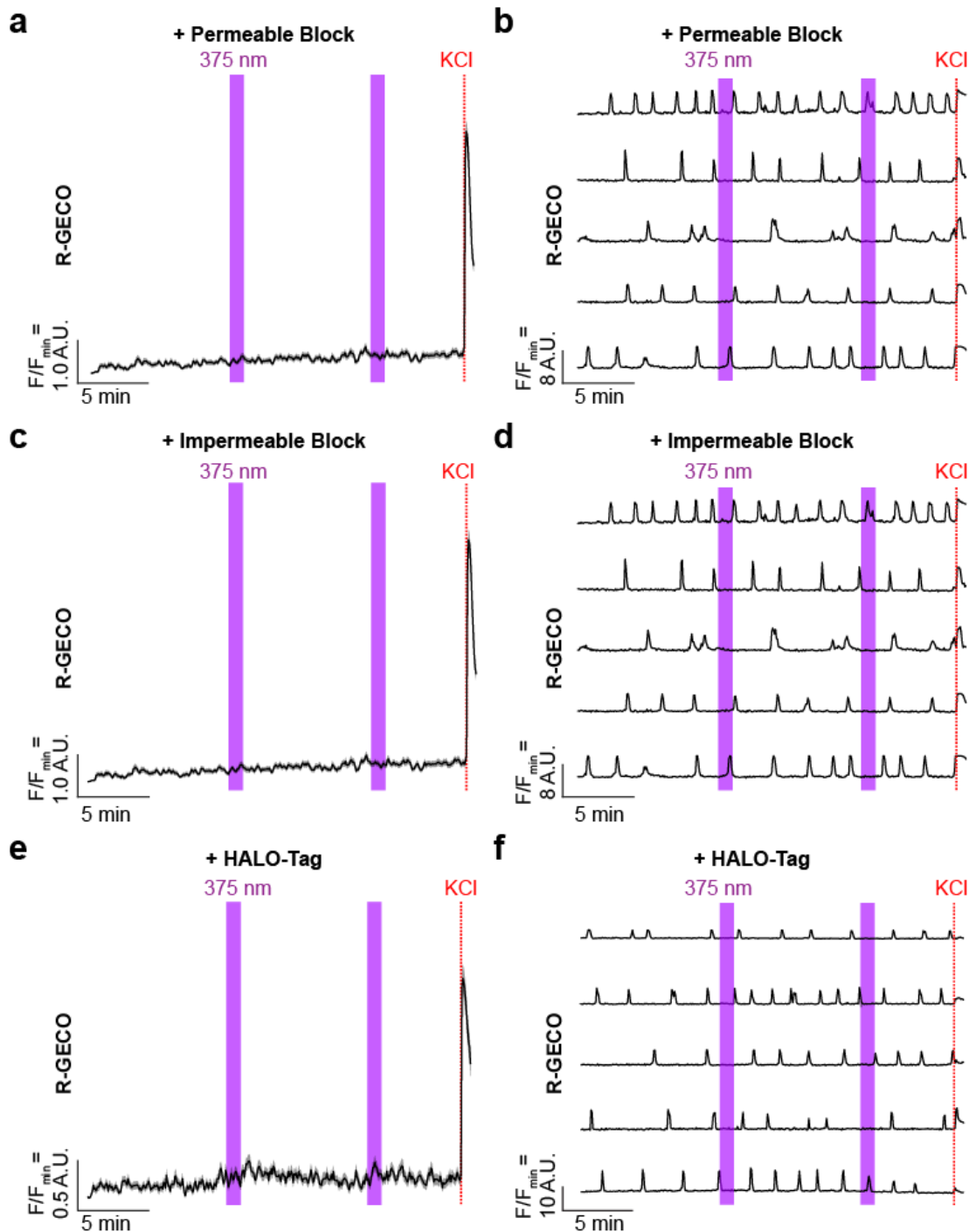


Figure S14. SNAP-tags are necessary for OCT-PEA targeting. Fluorescent Ca^{2+} imaging in INS-1 cells expressing R-GECO and pDisplayTM-SNAP revealed that preincubation with cell (a,b) permeable SNAP-Cell[®] Block (10 μM , 20 min, N = 248, T = 4) and (c,d) impermeable SNAP-Surface[®] Block (20 μM , 1 h, N = 278, T = 5) abolished the activity of OCT-PEA (5 μM , 2 h) uncaging. (e,f) Fluorescent Ca^{2+} imaging in INS-1 cells expressing R-GECO and pDisplayTM-HALO (N = 330, T = 4), showing that OCT-PEA (5 μM , 2 h) uncaging did not affect INS-1 Ca^{2+} oscillations. Displayed as (c) average and (d) representative traces from five cells. Shaded error bars = mean \pm S.E.M.

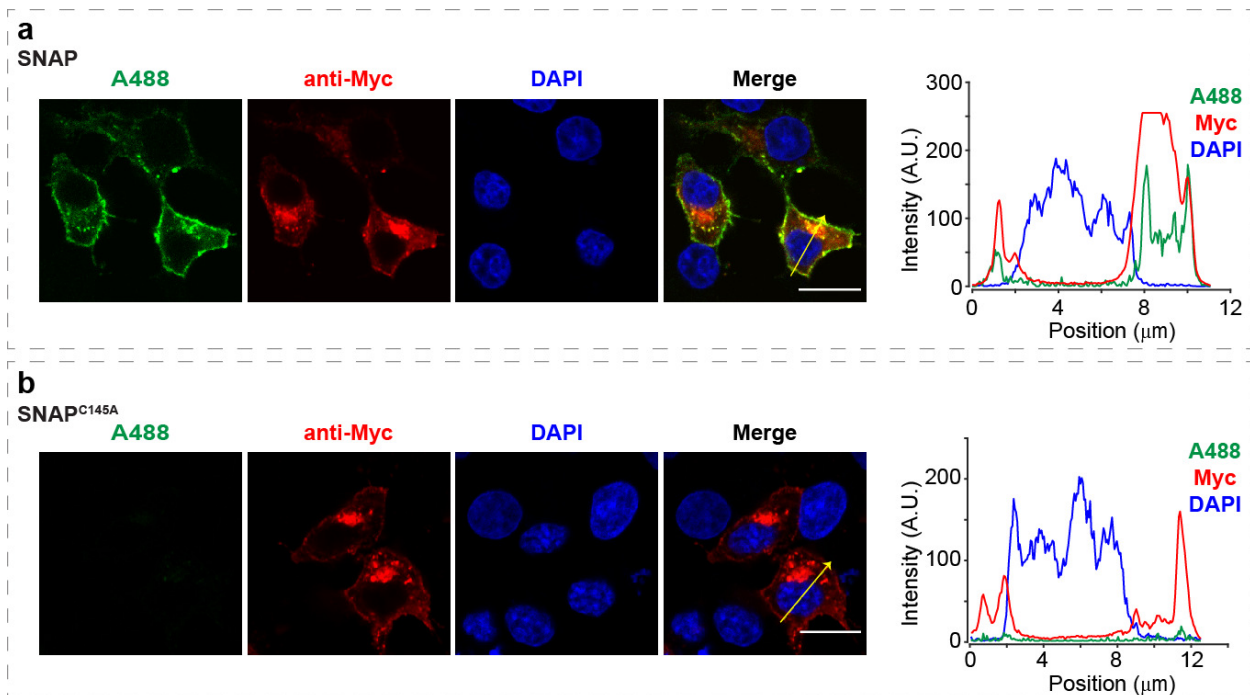


Figure S15. C145A SNAP-tag mutant maintains surface localization but does not recognize BG motif. Both pDisplayTM-SNAP and pDisplayTM-SNAP^{C145A} constructs contain a Myc-tag. **(a)** Images showing pDisplayTM-SNAP labeling with SNAP-Surface[®] Alexa Fluor[®] 488 (green), immunofluorescent staining of anti-MYC tag (red), and DAPI (blue). Intensity plot along the yellow line shown in the merge image. **(b)** Images showing pDisplayTM-SNAP^{C145A} labeling with SNAP Surface-Alexa488 (green), immunofluorescent staining of anti-MYC tag (red), and DAPI (blue). Intensity plot along the yellow line shown in the merge image. Scale bars = 10 μm .

SUPPLEMENTARY TABLES

Table S1: Corresponding primary and secondary antibodies for immunohistochemistry

Protein Target	Primary Antibody	Secondary Antibody
GPR55	GPR55 Rabbit polyclonal antibody (Bioss Antibodies, cat # BS-7686R, lot # VK3136032A); 1:200 dilution	Alexa Fluor 488 conjugated Donkey anti-Rabbit (Life Technologies, cat # A21206); 1:2000 dilution
Insulin	Insulin Guinea Pig polyclonal antibody (Abcam, cat # ab7842, lot #GR3322969-1); 1:250 dilution	IgG (H+L) Highly Cross-Adsorbed Goat anti-Guinea Pig, Alexa Fluor™ 594 (Invitrogen, cat # A11076, lot #2160074); 1:250 dilution
Myc-tag	Myc-tag Mouse mAB (Cell Signaling Technology, cat #2276, lot 24), 1:8000	Cy™3 AffiniPure Donkey anti-Mouse IgG (H+L) (Jackson ImmunoResearch Laboratories, cat #715-165-151, lot #130991), 1:1000

Table S2: Statistical significance calculations for fold change in oscillation frequency for PEA

	DMSO	PEA
DMSO	-	0.0072
PEA	0.0072	-
CID16020046	0.9361	0.0071
U73122	0.4640	0.0127
U73343	0.0190	0.8904

**P<0.01 (dark red), *P<0.05 (pink), ns = P>0.05 (white)

Table S3: Statistical significance calculations for fold change in oscillation frequency for OCT-PEA Ca²⁺ data

	DMSO	OCT-PEA
DMSO	-	0.0039
OCT-PEA	0.0039	-
CID16020046	0.1045	0.0184
U73122	0.4944	0.0051
U73343	0.0310	0.0911
S. Block	0.0400	0.0104
C. Block	0.0490	0.0084
SNAP ^{PC145A}	0.0238	0.0118
Halo	0.0583	0.0178

**P<0.01 (dark red), *P<0.05 (pink), ns = P>0.05 (white)

Table S4: siRNA GPR55 sequence and Catalog number

Abbreviation	Cat No. / Lot No.	5' → 3' Sequence
siRNA GPR55 A	10620318 – 439644 A06	CCUAUAGGAGCAUUCACAUUCUACU
siRNA GPR55 B	10620318 – 439644 B07	CCAUUGCUACCAAUCUUGUCGUCUU
siRNA Scramble	12935-200 Stealth RNAi™ siRNA Negative Control, Low GC Duplex	-

SUPPLEMENTARY METHODS

General synthetic methods

Unless otherwise noted, all chemicals were purchased from TCI Chemicals, Fisher Scientific, Sigma-Aldrich, or Acros Organics, and were used without further purification. Dry solvents were purchased as “extra dry” or “anhydrous” and used without further purification. Reactions and chromatography were monitored by analytical thin layer chromatography (TLC) on Merck silica gel 60 F₂₅₄ plates. The plates were first visualized under 254 nm UV light, followed by staining with KMnO₄ solution or cerium (IV) molybdate solution (Hanessian’s stain) and gentle heating with a heat gun. Flash column chromatography was performed using silica gel (ACROS Organics™ 240360300, 0.035-0.070 mm, 60 Å).

Nuclear magnetic resonance (NMR) spectra were acquired on a BRUKER 400 MHz instrument. Chemical shifts (δ) are reported in ppm and referenced to residual non-deuterated solvent peaks (¹H/¹³C): DMSO (2.50/39.52), MeOD (3.31/49.00), and CDCl₃ (7.26/77.16). Multiplicities are abbreviated as: s = singlet, d = doublet, t = triplet, q = quartet, br = broad, m = multiplet.

High-resolution (35,000) mass spectrometry was submitted to Portland State University’s BioAnalytical Mass Spectra Facility. Data were acquired on a vanquish UHPLC/HPLC system coupled to a Q-Exactive MS equipped with an electrospray ionization source operating in the positive mode.

UV-Vis spectroscopy

The sample was placed in a 1 mL Quartz cuvettes (10 mm light path) and illuminated with a deuterium-halogen light source (Ocean Optics, DH-2000). The transmitted light was collected by a Flame UV-Vis-ES spectrophotometer (FLMT05021, Ocean Insight) and the data were acquired with OceanView (Version 2.0.7) Software. Purified SNAP-tags (for Fig. S3) were purchased from New England Biolabs and labelled with our probes according to the manufacturer’s instructions. Uncaging was achieved using 365 nm, 415 nm, 470 nm, and 565 nm fibre-coupled LEDs (Thorlabs) guided through a fibre-optic cable (Thorlabs #FP400URT, 400 μ m diameter, 0.50 numerical aperture) and optical cannula (400 μ m, Thorlabs). The cannula tip was pointed directly into the top of the sample. LED power was quantified by a power meter (Thorlabs, PM100D) with its photodiode power sensor (Thorlabs, S120VC,) positioned directly at the fibre tip. OCT-PEA (20 μ M in DMSO) was irradiated for up to 5 min, and adsorption spectra were acquired every 2 s. When OCT-PEA was conjugated to SNAP-tag

purified protein, absorbance spectra were acquired every 5 s up to 10 min. The data were analyzed using MATLAB. Exponential curve fitting was achieved using Matlab's Curve Fitting application as:

$$f_t = a * e^{(-b*x)} + c$$

HPLC and HPLC-MS analysis

Analytical high-performance liquid chromatography (HPLC) kinetic analysis (as shown in Fig. S1b) was performed on a Varian ProStar HPLC with a Thermo Scientific™ Accucore™ C8 HPLC Column (2.6 μm, 150 × 4.6 mm). Solvent A = H₂O + 0.1% formic acid (FA); solvent B = acetonitrile + 0.1% FA. The gradient was from 45% B → 100% B over 15 min, followed by 100% B for 4 min, followed by 50% B for 1 min at 1 mL/min flow rate. The absorption was monitored at 280 and 320 nm with a ProStar325 UV-Vis Detector. Chromatograms were loaded into Galaxie Chromatography Software and the % caged was determined by calculating the AUC ratio of the caged molecule vs. the uncaged nitroso-aldehyde. Data was processed in Matlab using a mono exponential fit curve.

HPLC-MS analysis (as shown in Fig. S1c,d) was performed on an Agilent 1260 infinity II HPLC equipped with a DAD detector running on the Agilent OpenLab CDS Chemstation Edition software Rev.C01.10[201]. This was coupled to a Thermo scientific LTQ Velos mass spectrometer running on the Thermo Xcalibur 2.2 SP1.48 software. Spectra were acquired in positive electrospray ionization (ESI) mode.

Cell culture media and solutions

INS-1 media: RPMI 1640 with L-glutamine (Gibco, #11875-093) with 10% FBS, Penicillin-strep (1:100) and (in mM) 10 HEPES (Fisher, #BP310-500), 1 sodium pyruvate (Alfa Aesar, #A11148) 0.05 2-mercaptoethanol (BME, Sigma, #M3148).

Imaging buffer contains (in mM): 185 NaCl, 1.2 CaCl₂, 1.2 MgCl₂, 1.2 K₂HPO₄, 20 HEPES. Adjusted to pH 7.4 with NaOH. Glucose was supplemented accordingly at 3, 11 or 20 mM.

Phosphate buffer contains (in mM): 320 Na₂HPO₄ (Fisher, #BP332-500), 80 Na(H₂PO₄)•H₂O (Fisher, #S369-1). Adjusted pH to 7.4 with NaOH.

4% PFA: paraformaldehyde (2 g, Sigma-Aldrich, #158127), 0.2 M phosphate buffer (25 ml), deionized H₂O (25 ml). Adjusted pH to 7.4. Kept on ice until use (within 24 h).

Blocking buffer: Phosphate buffer saline (PBS, Gibco, #70013-032) with 10% w/v bovine serum albumin (Fisher, #BP1605-100, lot #182765), and 0.3% v/v triton X-100 (Fisher, #BP151-100).

Cell culture

INS-1 832/13 cells¹ were grown in INS-1 media and incubated at 37 °C and 5% CO₂. Cells between passages 60-80 were used in experiments. For Ca²⁺ imaging, INS-1 cells were plated at a density of 100,000-150,000 cells per well on 8-well glass bottom chambered coverslips (Ibidi, #0827-90). 18-24 h later, they were starved in Opti-MEM™ (250 µl) for 2 h. A transfection mixture containing (20 µl per well): 1 µl Lipofectamine-2000 (Fisher Scientific, #11668019), 250 ng R-GECO or 125 ng R-GECO + 250 ng pDisplay™-SNAP / 250 ng pDisplay™-HALO / 250 ng pDisplay™-SNAP^{C145A} in Opti-MEM™ was mixed and incubated for 20 min at room temperature. Following starvation, 230 µl fresh Opti-MEM™ was placed on the cells, followed by 20 µl transfection mixture. The cells were then incubated at 37 °C and 5% CO₂ for 18-24 h before exchanging the transfection mixture with INS-1 media. Microscopy experiments were performed 60-72 h post transfection.

Use of conditioned imaging buffer (supplements the INS-1 secreted factors) prior to Ca²⁺ imaging was necessary to achieve a stable baseline recording. The media on a separate petri dish of INS-1 cells (6 cm, 80% confluence) was exchanged for imaging buffer and incubated at 37 °C and 5% CO₂ for at least 1 h. This conditioned imaging buffer was added to the cells as the final wash directly before imaging.

For siRNA transfection, an siRNA (Invitrogen, Table S4): Oligofectamine™ (Invitrogen, #12252-011) complexes were prepared separately (1 µl of 20 µM siRNA : 16 µl Opti-MEM™ for siRNA complex and 0.8 µl Oligofectamine™ : 3 µl Opti-MEM™ for Oligofectamine™ complex per well) and incubated for 7 min at room temperature. The Oligofectamine™ complex mixture was added to the siRNA complex mixture and incubated together for 20 min at room temperature, then added to INS-1 cells freshly seeded at 100,000 cells per well on 8-well glass bottom chambered coverslips. INS-1 cells were transfected with R-GECO and pDisplay™-SNAP the following day as described above, and imaged 60-72 h post transfection.

cDNA constructs and site-directed mutagenesis

SNAP- and HALO-tags were inserted into the pDisplay™ vector (ThermoFisher #V66020) using Gibson cloning. Site-directed mutagenesis to create the C145A mutation of the pDisplay™-

SNAP construct was achieved using the QuikChange XL Site-Directed Mutagenesis Kit from Agilent Technologies with forward primer 5'-TTCTGATCCCGGCACACCGTGTGGT-3' and reverse primer 5'-ACCACACGGTGTGCCGGGATCAGAA-3'. After amplification, success of cloning was confirmed via Sanger sequencing.

Cell viability assay - MTT

INS-1 cells were plated in a 96-well plate (Corning #3596) with 50,000 cells per well in INS-1 media, and then were incubated for 48-72 h until they reached 70-80% confluence. For application of uncaged probe, OCT-PEA (10 μ l, 40 mM in DMSO) was irradiated for 5 min as described above in the "UV-Vis spectroscopy" section. The media in the 96-well plate of cells was exchanged with 100 μ l of INS-1 media with DMSO (0.1% v/v) and without BME. Afterwards, the compounds were added, and the cells were incubated at 37 °C and 5% CO₂ for 24 h. The media was aspirated from the wells and washed in 100 μ l PBS. 3-(4,5-Dimethyl-2-thiazolyl)-2,5-diphenyltetrazolium bromide (MTT, TCI Chemicals, #D0801) was added to the wells at 5 mg/ml and incubated at 37 °C and 5% CO₂ for 4 h. The media was gently removed and then 100 μ l DMSO was added to each well. The plate was placed in the dark on an orbital shaker for 15 min at 100 rpm. Absorbance at 590 nm was recorded on a CLARIOstar^{PLUS} plate reader (BMG Labtech, 0430) and the data were processed in Microsoft Excel and MATLAB.

Immunofluorescence microscopy

INS-1 cells were plated on acid-etched glass coverslips (12 mm, #1.5) at a density of 100,000 cells per well in a 24-well plate (Fisherbrand, #FB012929). The cells were fixed with ice-cold PFA (4%, 20 min, room temperature, orbital shaker 100 rpm), and then washed twice with PBS (5 min). Fixed INS-1 cells on coverslips were incubated in the blocking buffer (1 h). Cells were then incubated in 1° antibody solution (diluted in blocking buffer). The plate was sealed and incubated overnight (12-14 h, 4 °C, orbital shaker 100 rpm) in the dark. The coverslips were then washed three times with PBS (5 min, room temperature, orbital shaker 100 rpm). They were then transferred to the 2° antibody solution (diluted in blocking buffer, 1 h, room temperature) and shaken in the dark. Details of the specific antibodies and dilutions are provided in Table S1. The coverslips were washed three times with PBS (5 min) and then incubated in the dark with DAPI (Thermo, #D1206, 36 nM, 10 min) on the orbital shaker, and then washed twice with deionized water (5 min). The coverslips were mounted on a microscope slide (VWR® Superfrost® Plus Micro Slide, 75×25×1 mm, #48311-703) and sealed with

mounting solution (Fluoromount™). Slides remained in the dark overnight and then imaged within one week.

Fixed cell microscopy was performed on a Zeiss LSM880 confocal laser scanning microscope with Airyscan with a 63× oil objective at 2048×2048 resolution. DAPI excitation was performed with a 405 nm laser. Green fluorophores were excited with a 488 nm laser. Red fluorophores were excited with a 550 nm laser.

Live-cell confocal fluorescence microscopy

Live cell imaging was performed on an Olympus Fluoview 1200 laser scanning confocal microscope at 37 °C and 5% CO₂. Images were acquired with a 63× oil objective and 2048x2048 pixel resolution, and videos were acquired with a 20× objective, 512×512-pixel resolution, and scan rate of 4 s per frame. R-GECO excitation was performed with a 559 nm laser and emission was collected at 570-670 nm. SNAP-Surface® Alexa Fluor® 488 (NEB, #S9129S) excitation was performed with a 488 nm laser and emission was collected at 500-545 nm. Hoechst-33342 excitation was performed with a 405 nm laser and emission was collected at 425-460 nm. Photo-activation was performed with a 375 nm laser (PicoQuant, PDL 800-D, ~95 μW output from the objective) triggered using the quench function in the Olympus software.

For SNAP-tag dye labeling, the cells were washed once, labeled with SNAP-Surface® Alexa Fluor® 488 (1 μM, 30 min) in INS-1 media (without BME), washed once, then incubated with Hoechst-33342 (10 μM, 5 min) in 20 mM glucose imaging buffer. The cells were washed twice and imaged in 20 mM glucose imaging buffer. For OCT-PEA Ca²⁺ imaging, cells were incubated with OCT-PEA (5 μM, 2 h) in INS-1 media without BME at 37 °C and 5% CO₂. Control experiments involved incubation with CID16020046 (5 μM, 30 min, Tocris, #4959), U73122 (5 μM, 30 min, Tocris, #1268), U73343 (5 μM, 30 min, Tocris, #4133), or SNAP-Cell® Block (10 μM, 20 min, NEB, #S9106S) in INS-1 media without BME. Cells were washed, and equilibrated for at least 20 min with conditioned imaging buffer 37 °C and 5% CO₂.

Data analysis and code availability

For Ca²⁺ imaging experiments, regions-of-interest were manually drawn around oscillating cells using the Fiji software², and the resulting data were analyzed with MATLAB scripts written in-house. All data and codes used for analysis are available on request.

Unless otherwise described, all data are presented as mean ± S.E.M, which is calculated as:

$$\text{S. E. M.} = \frac{\text{standard deviation}}{\sqrt{N}}$$

For Ca^{2+} imaging experiments depicting the averages over time, N is the total number of cells (technical replicates over all videos), and T is the number of independent experiments (biological replicates). Oscillations were calculated in MATLAB using the 'findpeaks' function with an x threshold of 2 and y threshold of 1.25. Following cell selection, the total number of oscillations across the field of view was counted from the beginning of the video to the first stimulus (PEA addition, or UV-A irradiation in the case of OCT-PEA). Separately, the total number of oscillations were counted for over an equivalent time post-stimulation. The sum of the peaks was normalized against the number of cells per video (to quantify "oscillations per cell" for each trial and condition), and then the mean fold change for post/pre-stimulation was calculated alongside the S.E.M. In the case of these oscillation frequency counts, N is the number of independent trials (biological replicates). Statistical significance was assessed using Matlab (Mathworks). For the comparison between two groups in oscillation frequency analysis, Welch's two-sample t-test was used, with significance threshold placed at * $P < 0.05$, ** $P < 0.01$, ns = $P > 0.05$.

DETAILED SYNTHETIC METHODS

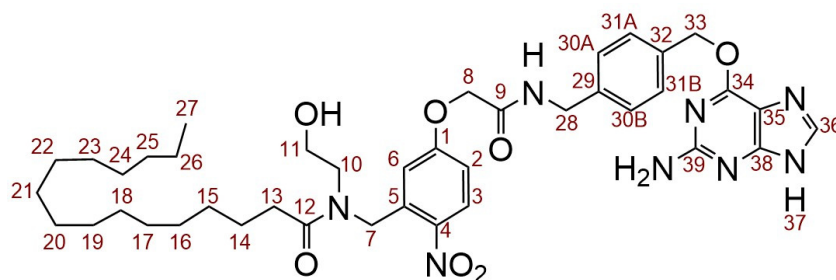
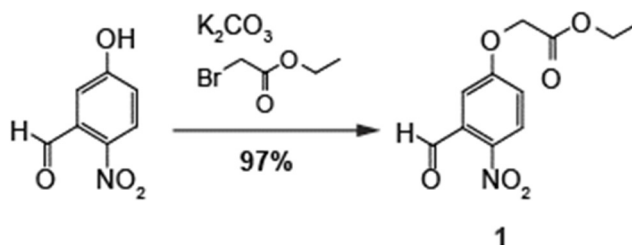


Figure S10 | Numbering system utilized in the following NMR assignments.

Ethyl 2-(3-formyl-4-nitrophenoxy) acetate (**1**)

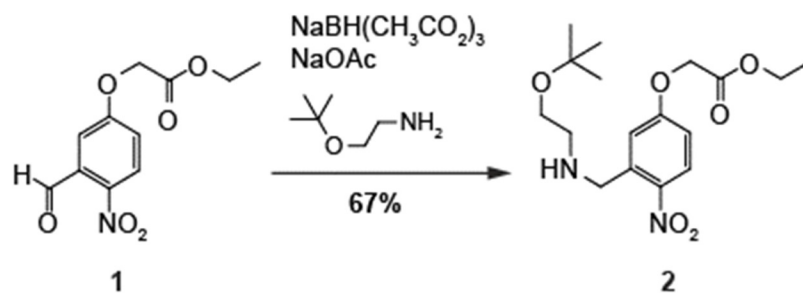


Ethyl 2-(3-formyl-4-nitrophenoxy) acetate (**1**) was prepared using a procedure as described by Heinbockel *et al.*³ 5-hydroxy-2-nitrobenzaldehyde (0.53 g, 3.2 mmol, 1.0 equiv.) and anhydrous K_2CO_3 (0.32 g, 2.3 mmol, 0.70 equiv.) were dissolved in dry acetonitrile (5 ml) under an Ar atmosphere. Ethylbromoacetate (0.40 ml, 3.6 mmol, 1.1 equiv.) was added dropwise and the reaction mixture was stirred overnight at room temperature. The reaction was filtered, and the filtrate was concentrated *in vacuo*. The residue was purified by flash column chromatography (hexane/EtOAc 95:5→80:20) to yield **ethyl 2-(3-formyl-4-nitrophenoxy) acetate (1)** (0.78 g, 3.1 mmol, 97%) as a yellow solid. Analytical data were comparable to those reported in Heinbockel *et al.*³

TLC (4:1 hexane:EtOAc): $R_f = 0.20$

1H NMR (CDCl₃, 400 MHz, 25° C): δ 10.48 (s, 1 H, CHO), 8.17 (d, 1 H, H3, $J = 9.1$ Hz), 7.31 (d, 1H, H6, $J = 3.0$ Hz), 7.20 (dd, 1 H, H2, $J = 8.8, 3.0$ Hz), 4.77 (s, 2 H, H8_{A,B}), 4.29 (q, 2 H, CH₂CH₃, $J = 7.1$ Hz), 1.32 (t, 3 H, CH₂CH₃, $J = 7.3$ Hz)

(2-*tert*-butoxyethyl)-(5-ethoxycarbonylmethoxy-2-nitrobenzyl)amine (2)

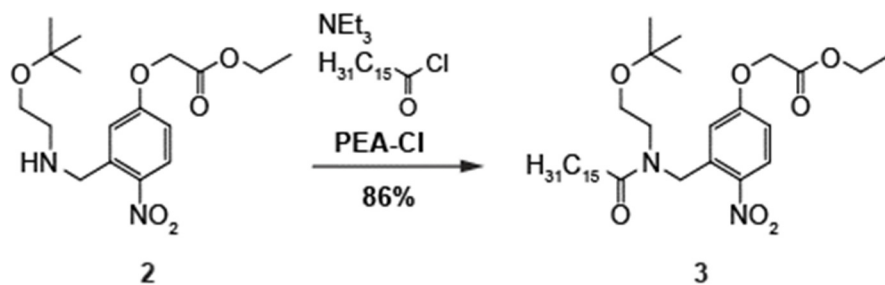


(2-*tert*-butoxyethyl)-(5-ethoxycarbonylmethoxy-2-nitrobenzyl)amine (**2**) was prepared as described by Heinbockel *et al.*³ 2-(*tert*-butoxy)-ethanamine (69 mg, 0.59 mmol, 1.5 equiv.) and ethyl 2-(3-formyl-4-nitrophenoxy) acetate (**1**) (0.10 g, 0.40 mmol, 1.0 equiv.) were dissolved in dry 1,2-dichloroethane (2 ml) under an Ar atmosphere. Anhydrous NaOAc (34 mg, 0.41 mmol, 1.0 equiv.) was then added, and the reaction mixture was stirred at room temperature for 1 h. $\text{NaBH}(\text{CH}_3\text{CO}_2)_3$ (0.21 g, 1.0 mmol, 2.5 equiv.) was added in one portion, and the reaction mixture was stirred overnight at room temperature. The reaction was diluted with CH_2Cl_2 (5 ml) and quenched with a saturated aqueous NaHCO_3 solution. The organic phase was separated, washed twice with a saturated aqueous NaHCO_3 solution, once with saturated brine, and then dried over anhydrous MgSO_4 . Following filtration and concentration *in vacuo*, the residue was purified *via* flash column chromatography (10 g silica, hexane/EtOAc 90:10→65:35 with 1 vol% Et_3N) to yield **(2-*tert*-butoxyethyl)-(5-ethoxycarbonylmethoxy-2-nitrobenzyl)amine (2)** (95 mg, 0.27 mmol, 67%) as a yellow oil. Analytical data were comparable to those reported in Heinbockel *et al.*³.

TLC (1:1 hexane:EtOAc): $R_f = 0.15$

$^1\text{H NMR}$ (CDCl_3 , 400 MHz, 25 °C): δ 8.08 (d, 1 H, H3, $J = 9.0$ Hz), 6.84 (dd, 1 H, H2, $J = 9.0, 2.9$ Hz), 4.71 (s, 2 H, H8_{A,B}), 4.28 (q, 2 H, CH_2CH_3 , $J = 7.1$ Hz), 4.13 (s, 2 H, H7_{A,B}), 3.49 (t, 2 H, H10_{A,B}, $J = 5.3$ Hz), 2.75 (t, 2 H, H11_{A,B}, $J = 5.3$ Hz), 1.73 (b, NH), 1.31 (t, 3 H, CH_2CH_3 , $J = 7.1$ Hz), 1.20 (s, 9 H, *t*-Bu CH_3)

***N*-(2-*tert*-butoxyethyl)-*N*-(5-ethoxycarbonylmethoxy-2-nitrobenzyl)palmitoylamide (**3**)**



Oxalyl chloride (0.36 ml, 4.2 mmol, 1.5 equiv.) was added to a solution of palmitic acid (0.7180 g, 2.8 mmol, 1.0 equiv.) in dry CH₂Cl₂ (35 ml) under an Ar atmosphere. A drop of *N,N*-dimethylformamide was added, and the reaction mixture was stirred for 70 min at room temperature. The reaction was concentrated *in vacuo* to yield a yellow-orange oil. To ensure complete removal of oxalyl chloride, the product was twice dissolved in CH₂Cl₂, concentrated *in vacuo*, and then dried under high vacuum (<1 mbar) for 20 min. The oil was dissolved in anhydrous CH₂Cl₂ (9 ml) immediately before use in the following reaction.

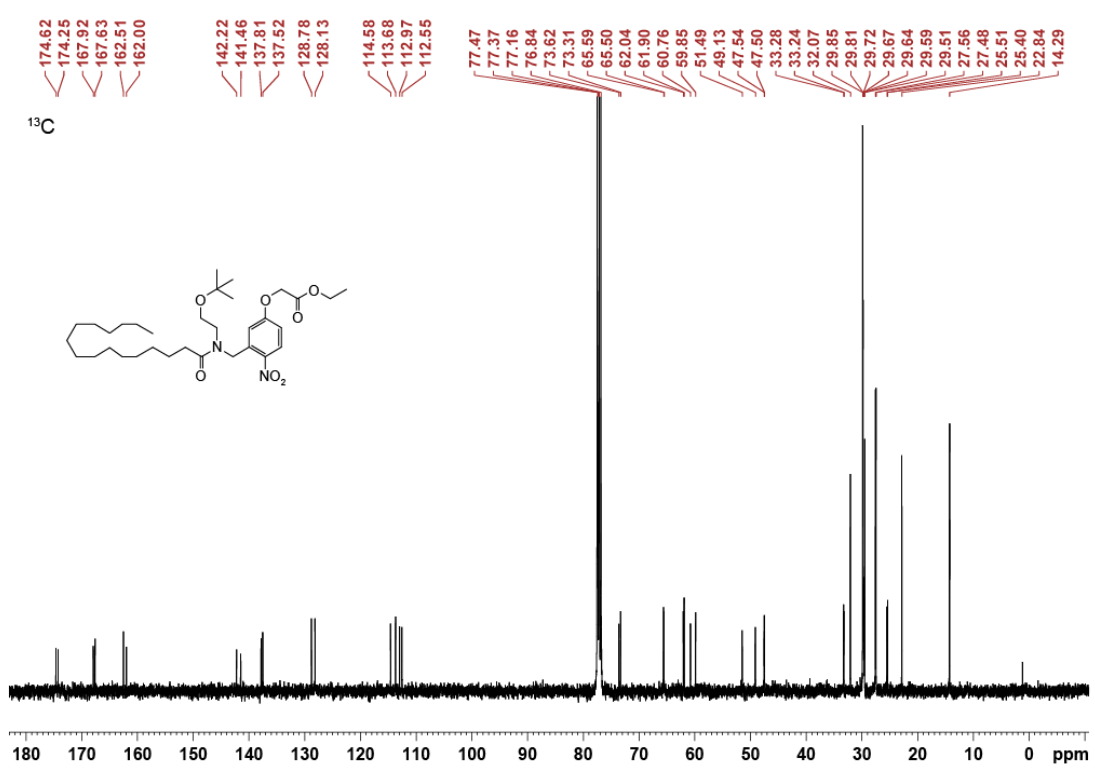
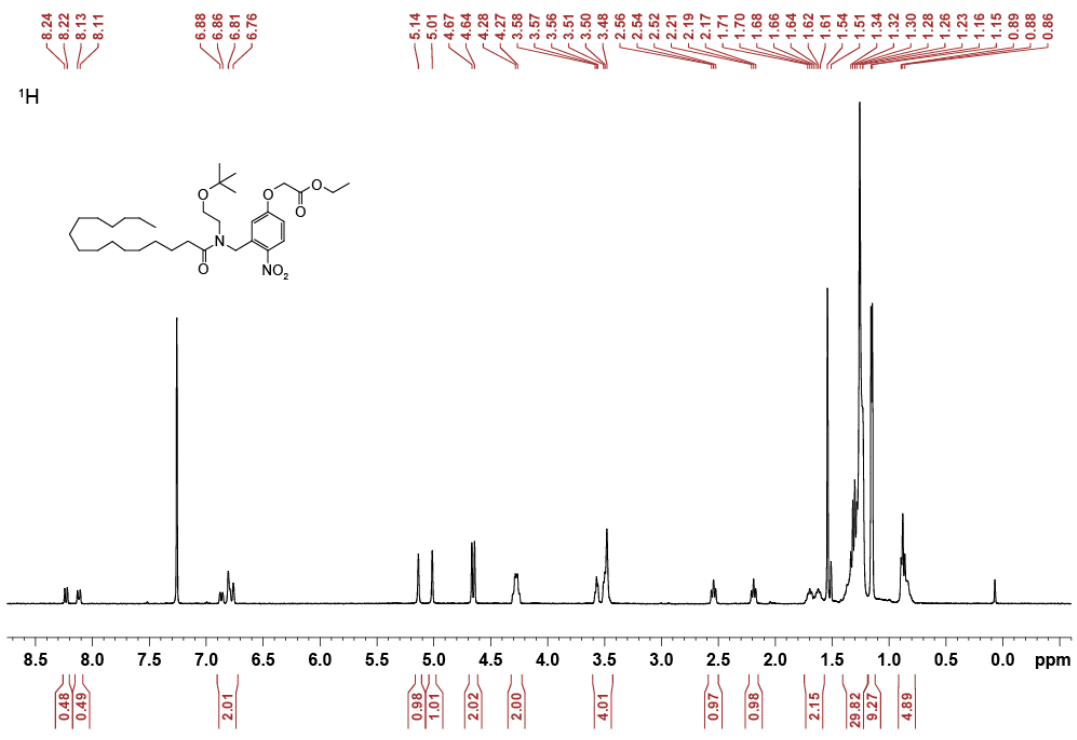
(2-*tert*-butoxyethyl)-(5-ethoxycarbonylmethoxy-2-nitrobenzyl)amine (**2**) (0.550 g, 1.6 mmol, 1.0 equiv.) was dissolved in dry CH₂Cl₂ (30 ml) under an Ar atmosphere, followed by dropwise addition of the above described palmitoyl chloride solution (9 ml, 1.8 equiv.) and then Et₃N (0.39 ml, 2.8 mmol, 1.8 equiv.). The reaction mixture was stirred for 90 min at room temperature, then diluted with CH₂Cl₂ (20 ml). The organic phase was washed twice with a saturated aqueous NaHCO₃ solution, once with saturated brine, and then dried over anhydrous MgSO₄. Following filtration and concentration *in vacuo*, the residue was purified *via* flash column chromatography (50 g silica, hexane/EtOAc 95:5→90:10→85:15), to yield ***N*-(2-*tert*-butoxyethyl)-*N*-(5-ethoxycarbonylmethoxy-2-nitrobenzyl)palmitoylamide (**3**)** (0.8197 g, 1.38 mmol, 86%), as a yellow oil. The product was isolated as a mixture of *E* and *Z* amide isomers.

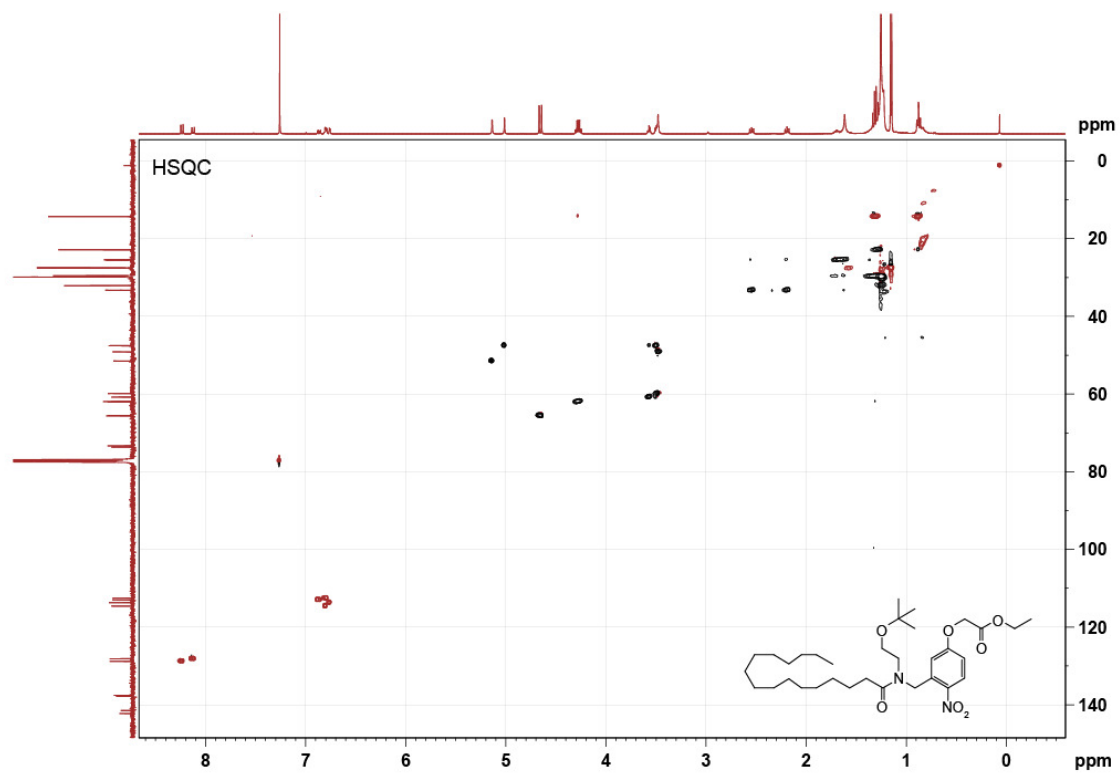
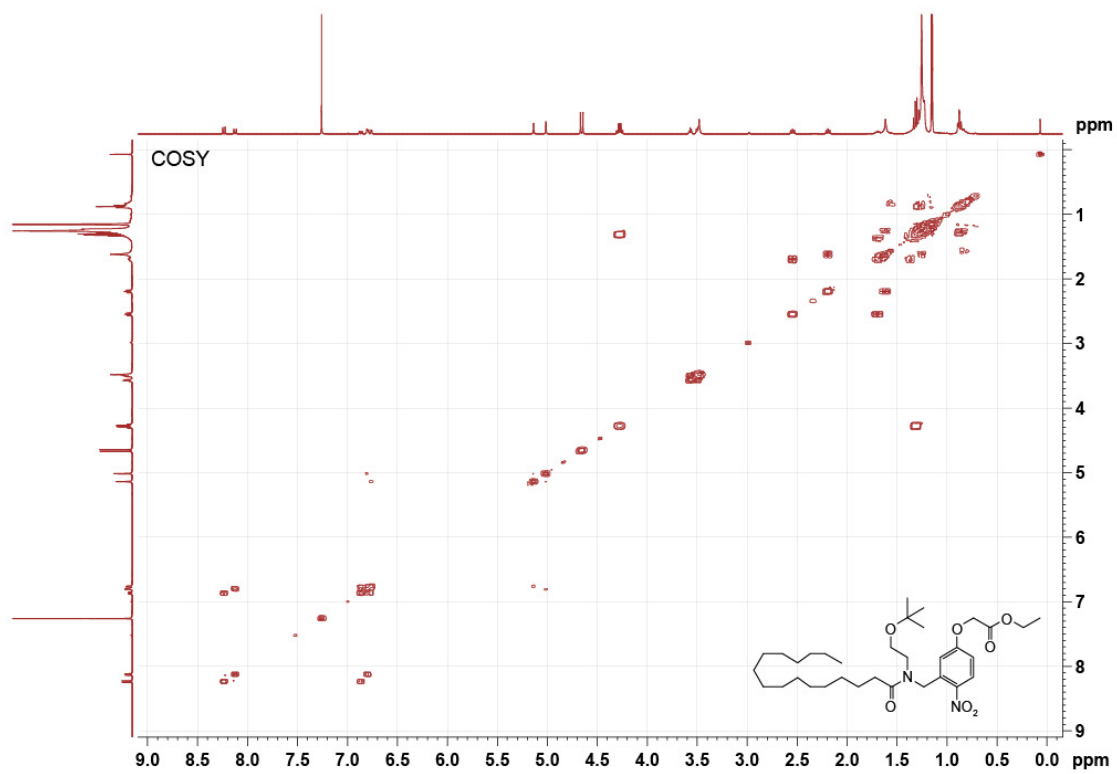
TLC (3:1 hexane:EtOAc): $R_f = 0.35$

$^1\text{H NMR}$ (CDCl_3 , 400 MHz, 25 °C): δ 8.23 (d, 0.5 H, H3, $J = 9.3$ Hz), 8.12 (d, 0.5 H, H3, $J = 9.5$ Hz), 6.91-6.72 (m, 2 H, H2, H6), 5.14 (s, 1 H, H7_A), 5.01 (s, 1 H, H7_B), 4.66 (d, 2 H, H8_{A,B}, $J = 9.5$ Hz), 4.32-4.23 (m, 2 H, CH_2CH_3), 3.60-3.43 (m, 4 H, H10_{A,B}, H11_{A,B}), 2.54 (t, 1 H, H13_A, $J = 7.6$ Hz), 2.19 (t, 1 H, H13_B, $J = 7.6$ Hz), 1.75-1.57 (m, 2 H, H14_{A,B}), 1.41-1.19 (m, 24 H, H15-H26, CH_2CH_3), 1.16 (d, 9H, *t*-Bu CH_3 , $J = 4.3$ Hz), 0.88 (t, 3H, H27_{A,B,C})

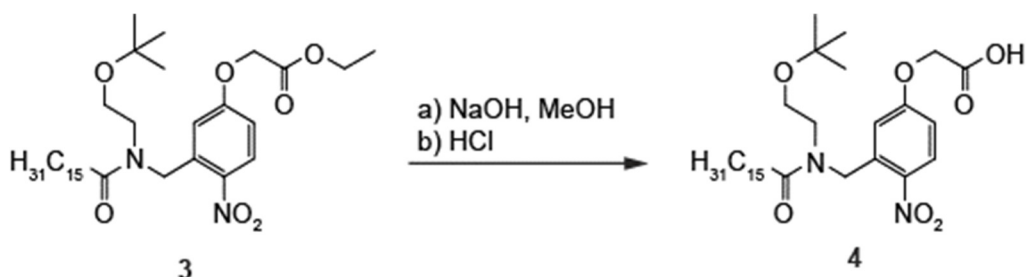
$^{13}\text{C NMR}$ (CDCl_3 , 101 MHz, 25 °C): δ 174.62 + 174.25 (C12), 167.92 + 167.63 (C9), 162.51 + 162.00 (C1), 142.22 + 141.46 (C4), 137.81 + 137.52 (C5), 128.78 + 128.13 (C3), 114.58 + 113.68 (C6), 112.97 + 112.55 (C2), 73.62 + 73.31 ($\text{C}(\text{CH}_3)_3$), 65.59 + 65.50 (C8), 62.04 + 61.90 (CH_2CH_3), 60.76 + 59.85 (C10, C11), 51.49 (C7), 49.13-47.50 (C10, C11), 33.28 + 33.24 (C13), 32.07-29.51 (C15-C26), 27.56 + 27.48 ($\text{C}(\text{CH}_3)_3$), 25.51 + 25.40 (C14), 22.84 (CH_2CH_3), 14.29 + 14.27 (C27)

HRMS (ESI⁺): m/z calculated for $[\text{C}_{33}\text{H}_{56}\text{N}_2\text{O}_7]^+$ = 593.4160, observed = 593.4149 ($[\text{M}+\text{H}]^+$)



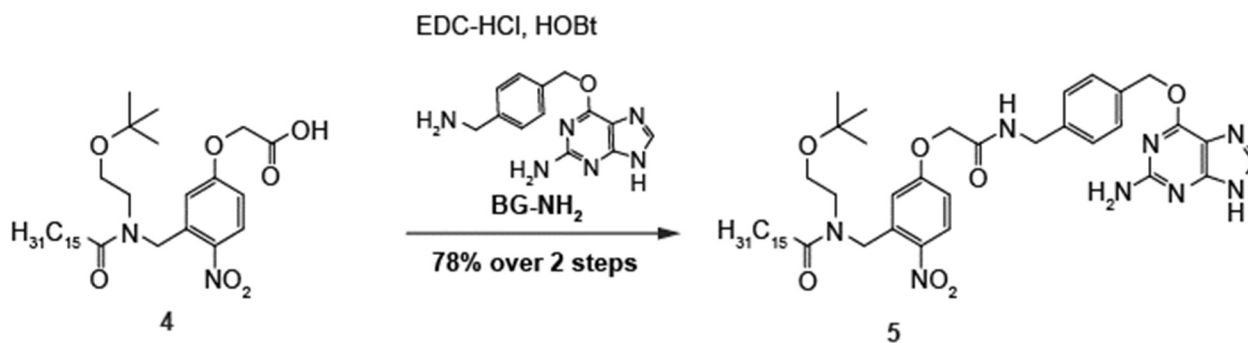


***N*-(2-*tert*-butoxyethyl)-*N*-(5-carboxymethoxy-2-nitrobenzyl)palmitoylamide (4)**



N-(2-*tert*-butoxyethyl)-*N*-(5-ethoxycarbonylmethoxy-2-nitrobenzyl)palmitoylamide (**3**) (0.5486 g, 0.93 mmol, 1.0 equiv.) was dissolved in MeOH (7.4 ml) and cooled in an ice-water bath for 5 min. 1 M aqueous NaOH (2 ml, 2 mmol, 2.0 equiv.) was added dropwise over 3 min, and the reaction continued for 1 h while gradually warming to room temperature. The reaction was again cooled in an ice-water bath and then neutralized with 1 M HCl (1.5 ml, 1.5 mmol, 1.5 equiv.). The reaction was diluted in EtOAc (5 ml), and the aqueous phase was twice back-extracted with EtOAc and twice with Et₂O. The combined organic extracts were then washed twice with brine and dried over anhydrous MgSO₄. Filtration and concentration *in vacuo* yielded ***N*-(2-*tert*-butoxyethyl)-*N*-(5-carboxymethoxy-2-nitrobenzyl)palmitoylamide (4)** (0.552 g) as a white powder, which was immediately used in the next step without purification.

***N*-(2-*tert*-butoxyethyl)-*N*-(5-methoxy-6-((4-(aminomethyl)benzyl)oxy)-9*H*-purin-2-carbamoyl-2-nitrobenzyl)palmitoylamide (5)**



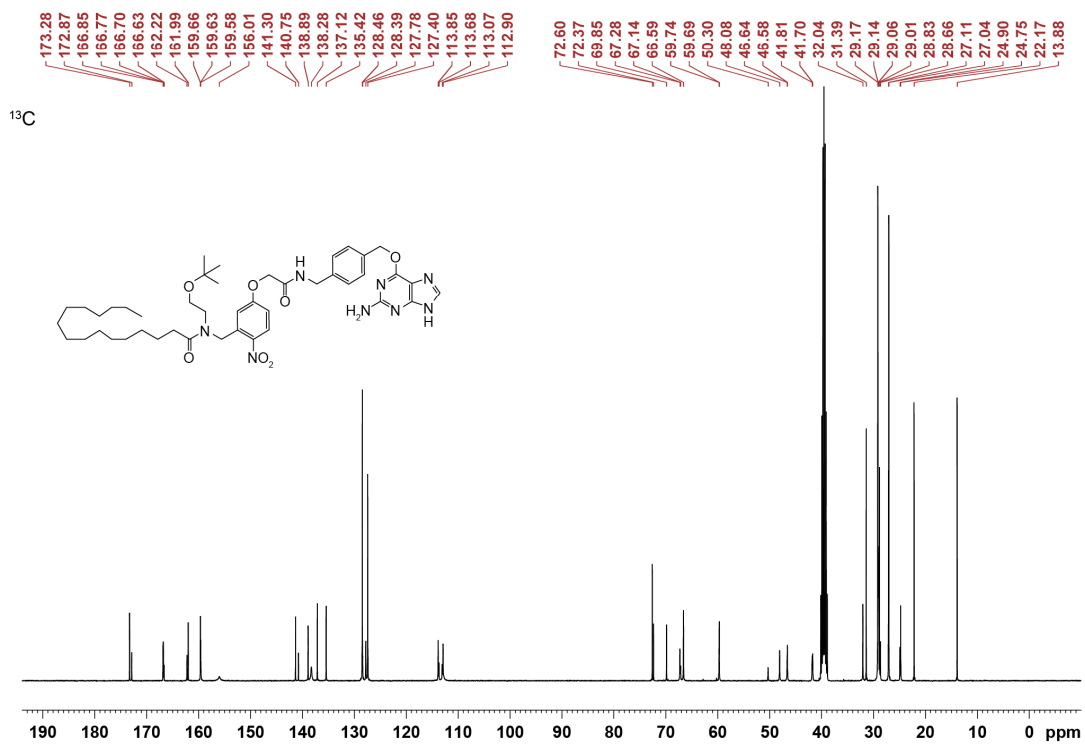
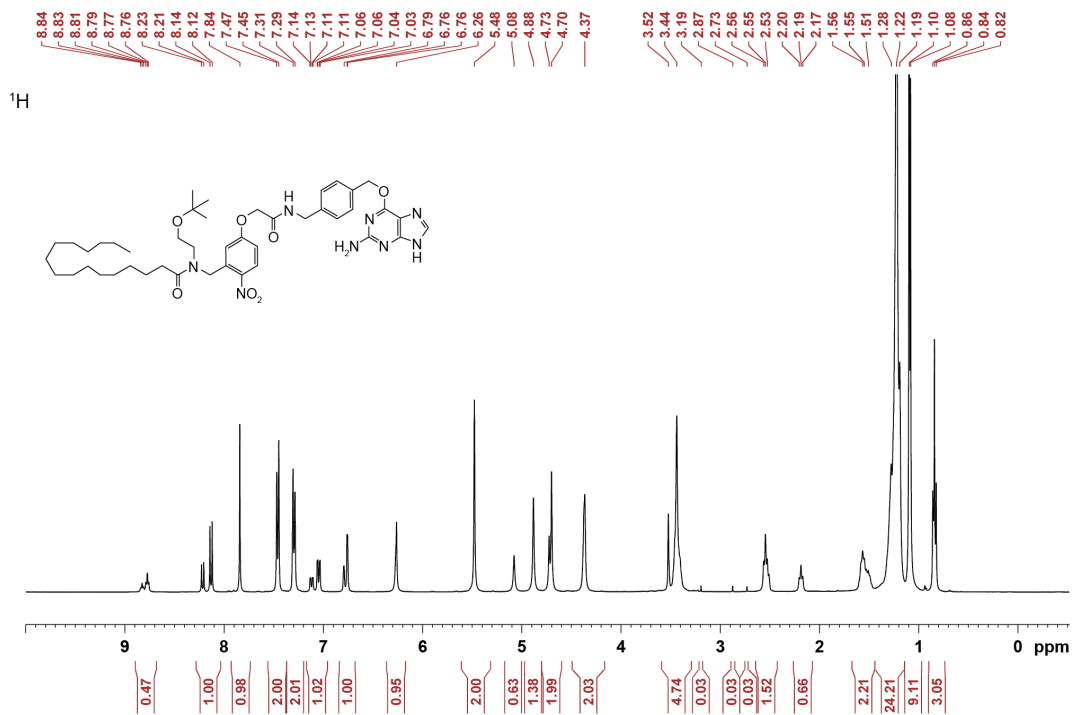
6-((4-(aminomethyl)benzyl)oxy)-9*H*-purin-2-amine (BG-NH₂) was prepared using a procedure described in Keppler *et al.*⁴ 1-hydroxybenzotriazole (HOBT) (0.1492 g, 1.1 mmol, 1.1 equiv.) and 1-(3-dimethylaminopropyl)-3-ethylcarbodiimide hydrochloride (EDC-HCl) (0.2126 g, 1.1 mmol, 1.1 equiv.) were added to *N*-(2-*tert*-butoxyethyl)-*N*-(5-carboxymethoxy-2-nitrobenzyl)palmitoylamide (**4**) (0.552 g, 0.98 mmol, 1.0 equiv.). The mixture was dissolved in dry *N,N*-dimethylformamide (30 ml) under an Ar atmosphere and was stirred for 45 min in an ice-water bath. Separately, BG-NH₂ (0.336 g, 1.24 mmol, 1.3 equiv.) was dissolved in dry *N,N*-dimethylformamide (15 ml) under an Ar atmosphere. The BG-NH₂ solution was added dropwise to the reaction flask over 15 min and stirred overnight, while slowly warming to room temperature. After diluting the reaction in EtOAc (40 ml), the organic phase was washed twice with a saturated aqueous NaHCO₃ solution (100 ml), twice with 0.1 M aqueous HCl (100 ml), twice with H₂O (100 ml), and once with saturated brine. The organic phase was dried over anhydrous MgSO₄, filtered, and then concentrated *in vacuo*. The residue was purified *via* flash column chromatography (60.12 g silica, CH₂Cl₂/MeOH 99:1→97:3→95:5) to yield ***N*-(2-*tert*-butoxyethyl)-*N*-(5-methoxy-6-((4-(aminomethyl)benzyl)oxy)-9*H*-purin-2-carbamoyl-2-nitrobenzyl)palmitoylamide (5)** (0.5861 g, 0.72 mmol, 78% over two steps) as a yellow oil. The product was isolated as a mixture of *E* and *Z* amide isomers.

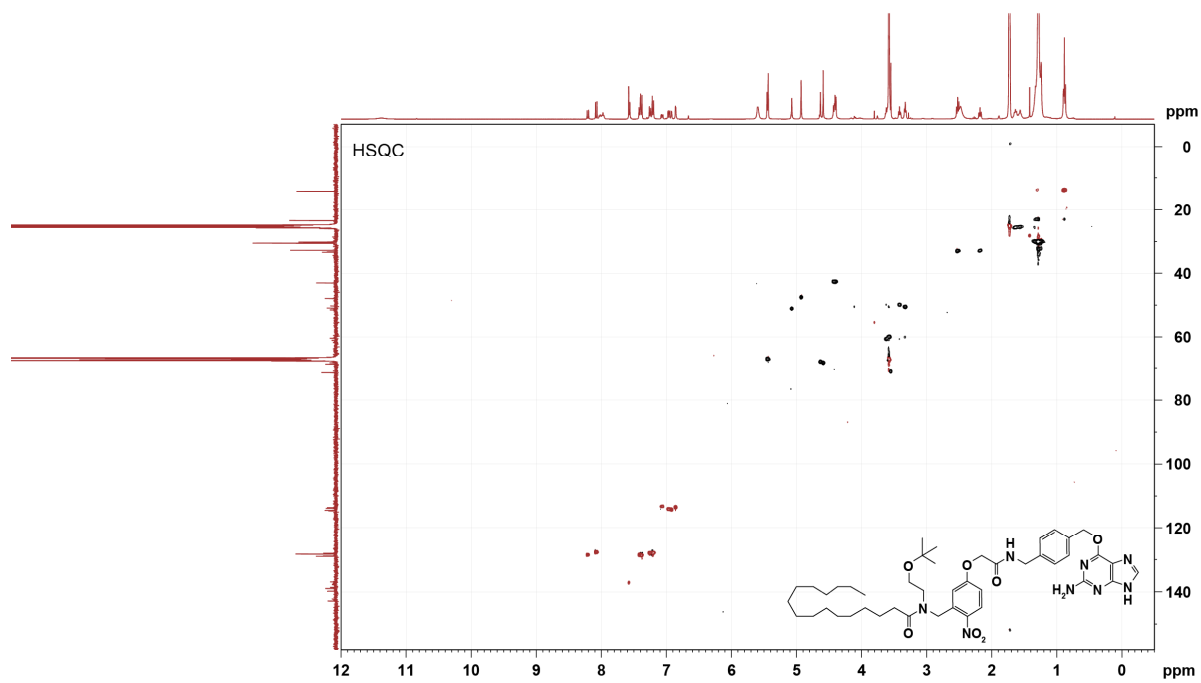
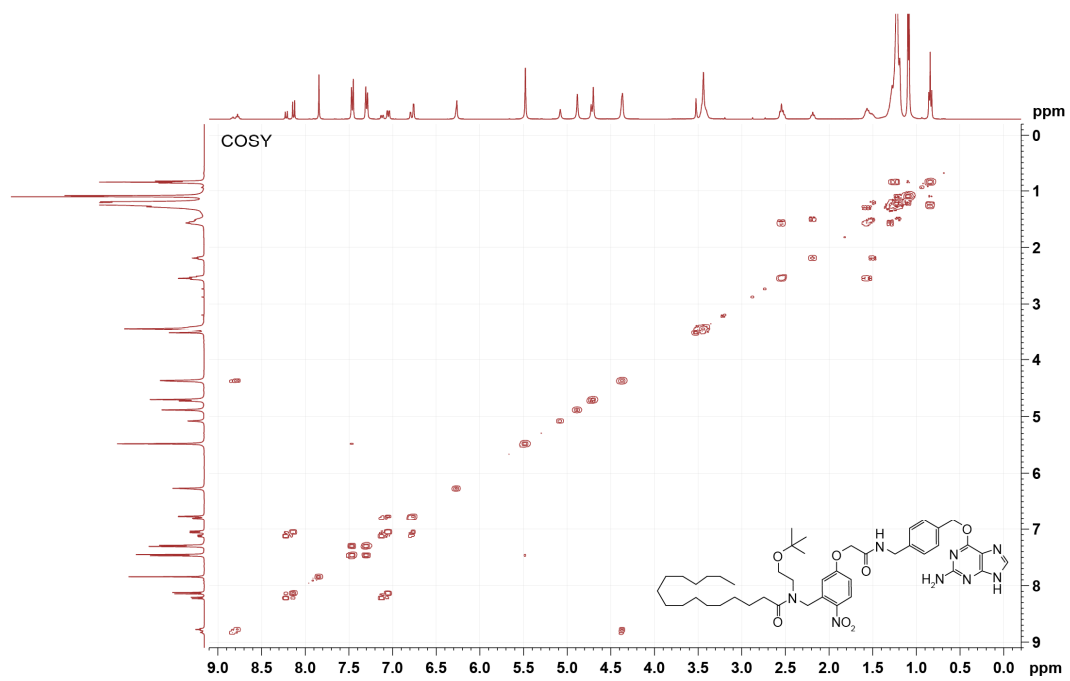
TLC (95:5 CH₂Cl₂:MeOH): R_f = 0.36

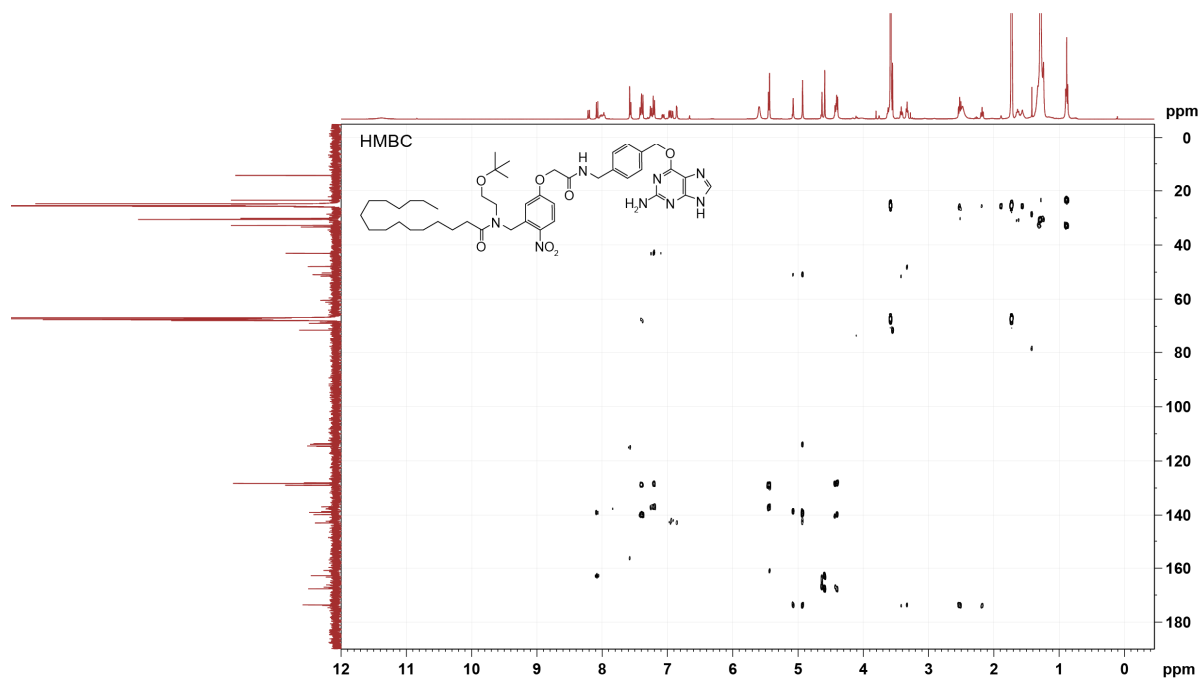
¹H NMR (DMSO, 400 MHz, 25 °C): δ 8.90-8.68 (m, 1.0 H, CONH), 8.22 (d, 0.3 H, H3, *J* = 9.0 Hz), 8.13 (d, 0.7 H, H3 *J* = 9.3 Hz), 7.84 (s, 1 H, H36), 7.46 (d, 2 H, H31_{A,B}, *J* = 8.1 Hz), 7.30 (d, 2 H, H30_{A,B}, *J* = 8.1 Hz), 7.09 (dd, 0.3 H, H2, *J* = 9.1, 2.8 Hz), 7.05 (dd, 0.7 H, H2, *J* = 9.0, 2.7 Hz), 6.79 (d, 0.3 H, H6, *J* = 2.4 Hz), 6.76 (d, 0.7 H, H6, *J* = 2.4 Hz), 6.26 (s, 1 H, NH), 5.48 (s, 2 H, H33_{A,B}), 5.08 (s, 0.6 H, H7_A), 4.89 (s, 1.4 H, H7_{A,B}), 4.70 (s, 2 H, H8_{A,B}), 4.37 (s, 2 H, H28_{A,B}), 3.44 (s, 4 H, H10_{A,B}, H11_{A,B}), 2.54 (t, 1.5 H, H13_{A,B}, *J* = 7.1 Hz), 2.19 (t, 0.7 H, H13_B, *J* = 7.0 Hz), 1.67-1.45 (m, 2 H, 14_{A,B}), 1.44-1.13 (m, 24 H, H15-H26), 1.09 (d, 9 H, *t*-Bu CH₃, *J* = 5.4 Hz), 0.84 (t, 3 H, H27_{A,B,C}, *J* = 6.8 Hz)

¹³C NMR (DMSO, 101 MHz, 25 °C): δ 173.28 (C12), 166.85 (C9), 161.99 (C1), 159.63 (C34), 141.30 (C4), 138.89 (C29), 138.28 (C36), 137.12 (C5), 135.42 (C32_{E/Z}), 128.46 (3 C, C32_{E/Z}, C30_{A,B}), 127.78 (C3), 127.40 (3 C, C29, C31_{A,B}), 113.85 (C6), 112.90 (C2), 72.60 (C(CH₃)₃), 667.28 (C8), 66.59 (C33), 59.69 (2 C, C10, C11), 46.58 (C7), 41.70 (C28), 32.04 (C13), 31.39 + 29.17 + 22.17 (12 C, C15-C26), 27.0371 (C(CH₃)₃), 24.75 (C14), 13.88 (C27)

HRMS (ESI⁺): *m/z* calculated for [C₄₄H₆₄N₈O₇]⁺ = 817.4971, observed = 817.4951 ([M+H]⁺)







***N*-(ethyl-2-ol)-*N*-(5-methoxy-6-((4-(aminomethyl)benzyl)oxy)-9*H*-purin-2-carbamoyl-2-nitrobenzyl)palmitoylamide (OCT-PEA)**



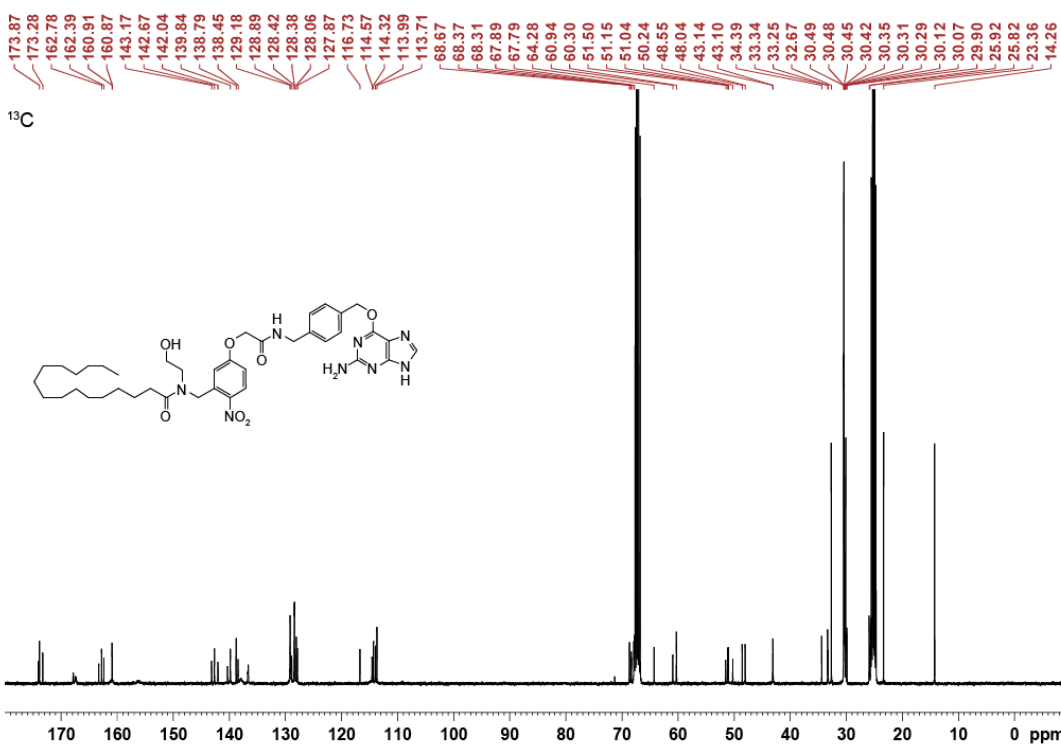
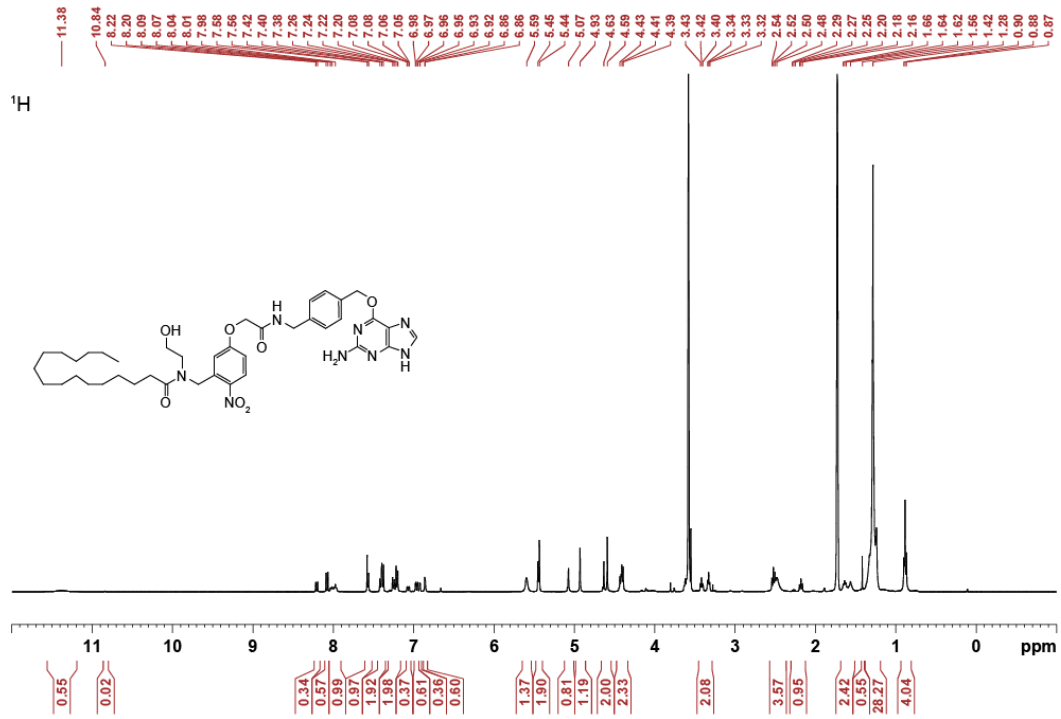
N-(2-*tert*-butoxyethyl)-*N*-(5-methoxy-6-((4-(aminomethyl)benzyl)oxy)-9*H*-purin-2-carbamoyl-2-nitrobenzyl)palmitoylamide (**5**) (0.1145 g, 0.14 mmol, 1.0 equiv.) was dissolved in dry CH_2Cl_2 (6.5 ml) under an Ar atmosphere, and then cooled in a dry ice / acetone bath. BBr_3 (1 M in CH_2Cl_2 , 0.56 ml, 0.56 mmol, 4 equiv.) was added over 5 min and the reaction continued for 50 min. The reaction was quenched with 4:1 $\text{MeOH}:\text{Et}_2\text{O}$ (3 ml), and stirred vigorously for 5 min. The reaction mixture was neutralized with Et_3N (0.3 ml, 2.1 mmol) and diluted in CH_2Cl_2 (42 ml). The reaction mixture was washed twice with H_2O (50 ml) and twice with saturated brine (50 ml). The organic phase was concentrated *in vacuo* and purified *via* flash column chromatography (15 g silica, $\text{CH}_2\text{Cl}_2/\text{MeOH}$ 93:7), yielding compound ***N*-(ethyl-2-ol)-*N*-(5-methoxy-6-((4-(aminomethyl)benzyl)oxy)-9*H*-purin-2-carbamoyl-2-nitrobenzyl)palmitoylamide (OCT-PEA**, 0.0627 g, 82 μmol , 59%) as a yellow oil. The product was isolated as a mixture of *E* and *Z* amide isomers.

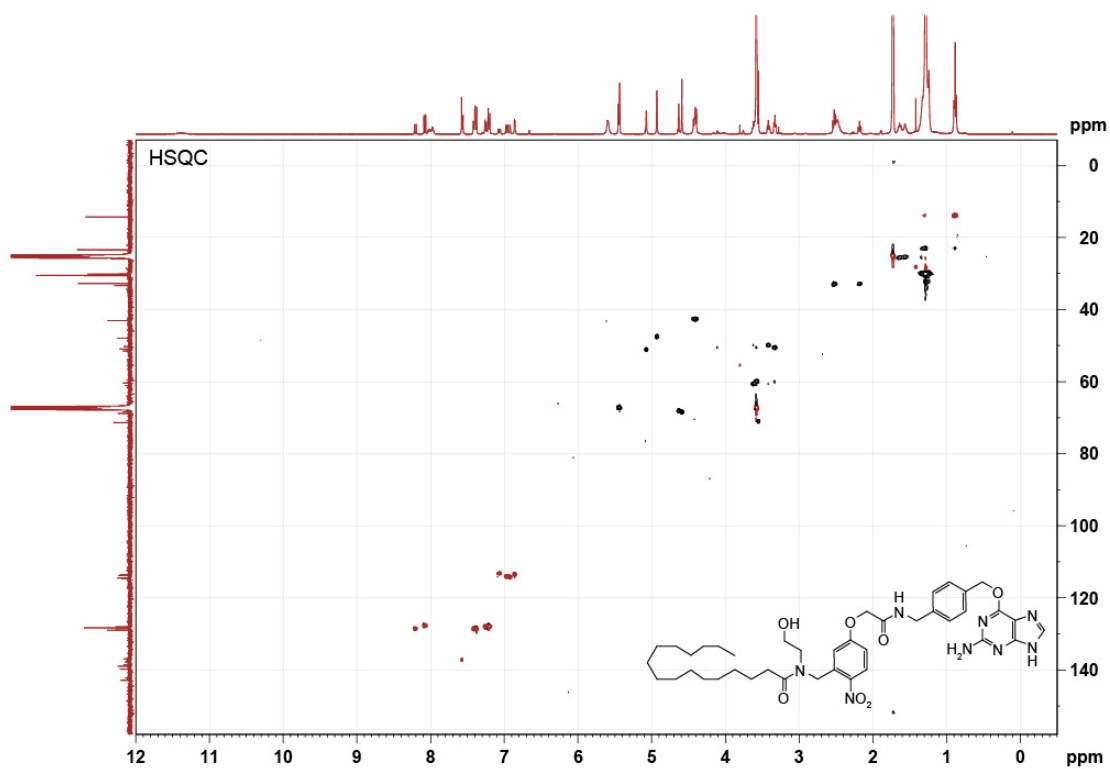
TLC (9:1 CH₂Cl₂:MeOH): R_f = 0.40

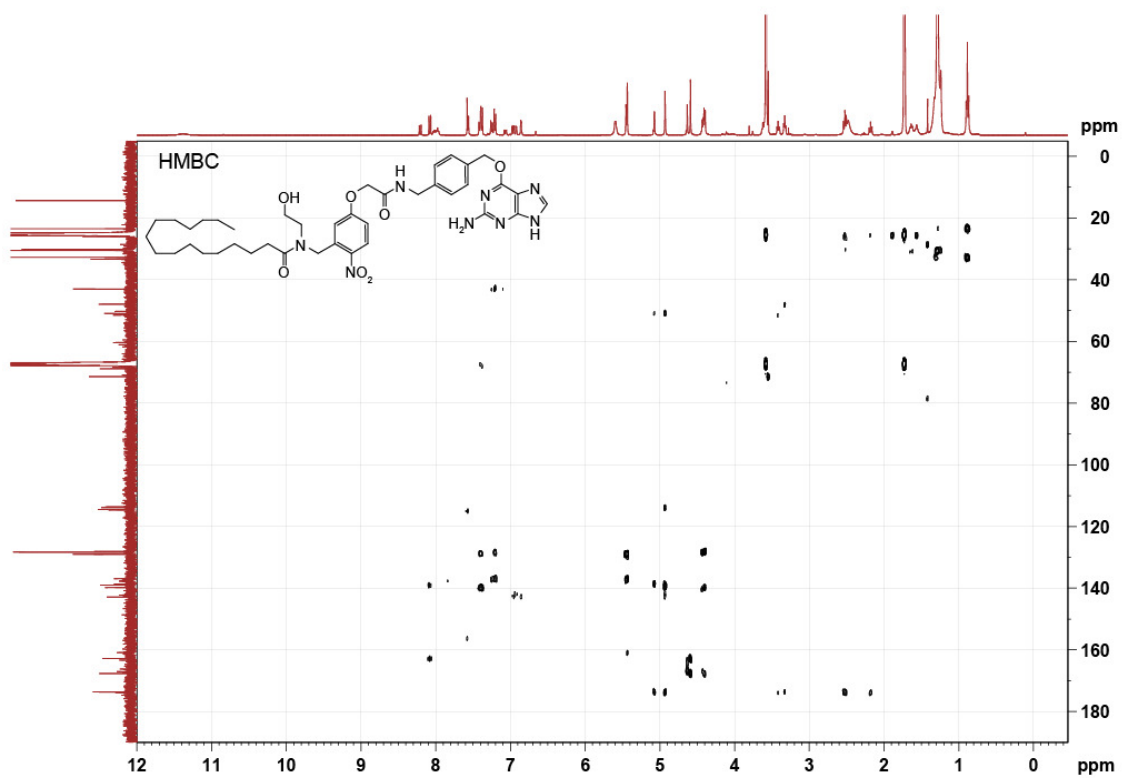
¹H NMR (THF, 400 MHz, 25 °C): δ 11.38 (b), 8.21 (d, 0.3 H, H3, *J* = 9.2 Hz), 8.08 (d, 0.6 H, H3, *J* = 9.5 Hz), 8.05-7.91 (m, 1 H, HNCO), 7.57 (d, 1 H, H36, *J* = 7.9 Hz), 7.40 (t, 2 H, H31_{A,B}, *J* = 8.7 Hz), 7.32 (dd, 2 H, H30_{A,B}, *J* = 17.9, 7.7 Hz), 7.07 (dd, 0.4 H, H2, *J* = 9.2, 2.6 Hz), 6.96 (dd, 0.6 H, H2, *J* = 9.2, 2.6 Hz), 6.92 (d, 0.4 H, H6, *J* = 2.3 Hz), 6.86 (d, 0.6 H, H6, *J* = 2.3 Hz), 5.59 (b), 5.44 (d, 2 H, H33, *J* = 6.9 Hz), 5.07 (s, 0.8 H, H7_A), 4.93 (s, 1.2 H, H7_{A,B}), 4.61 (d, 2 H, H8_{A,B}, *J* = 17.1 Hz), 4.48-4.34 (m, 2 H, H28_{A,B}), 3.46-3.29 (m, 2 H, H10_A/H11_A), 2.52 (t, H13_A, *J* = 7.4 Hz), 2.31-2.13 (m, 1 H, H13_B), 1.69-1.51 (m, 2 H, H14_{A,B}), 1.38-1.19 (m, 24 H, H15-H26), 0.88 (t, 3 H, H27_{A,B,C}, *J* = 6.7 Hz)

¹³C NMR (THF, 101 MHz, 25 °C): δ 173.87 (C12_{E/Z}), 173.28 (C12_{E/Z}), 167.86 (C9_{E/Z}), 167.34 (C9_{E/Z}), 162.78 (C1), 142.67 (C5), 138.79 (C4), 138.02 (C36), 136.62 (C32), 129.18 (2 C, C31_{A,B}), 128.89 (C3_{E/Z}), 128.42 (3 C, C29 + C30_{A,B}), 128.06 (C3_{E/Z}), 114.32 (C6_{E/Z}), 113.99 (C6_{E/Z}), 113.71 (C2_{E/Z}), 68.67 (C28), 68.37 (C8), 60.94 (C(CH₃)₃), 51.50 (C7_{E/Z}), 51.04 (C10), 50.24 (C11), 48.04 (C7_{E/Z}), 43.10 (C28), 33.34 (C13), 33.25 + 30.49 + 23.36 (12 C, C15-C26), 14.26 (C27)

HRMS (ESI⁺): *m/z* calculated for [C₄₀H₅₆N₈O₇]⁺ = 761.4345, observed = 761.4341 ([M+H]⁺)







References

- 1 H. E. Hohmeier, H. Mulder, G. Chen, R. Henkel-Rieger, M. Prentki and C. B. Newgard, *Diabetes*, 2000, **49**, 424–430.
- 2 J. Schindelin, I. Arganda-Carreras, E. Frise, V. Kaynig, M. Longair, T. Pietzsch, S. Preibisch, C. Rueden, S. Saalfeld, B. Schmid, J. Y. Tinevez, D. J. White, V. Hartenstein, K. Eliceiri, P. Tomancak and A. Cardona, *Nat. Methods*, 2012, **9**, 676–682.
- 3 T. Heinbockel, D. Brager, C. Reich, J. Zhao, S. Muralidharan, B. Alger and J. Kao, *J. Neurosci.*, 2005, **25**, 9449–9459.
- 4 A. Keppler, S. Gendreizig, T. Gronemeyer, H. Pick, H. Vogel and K. Johnsson, *Nat. Biotechnol.*, 2003, **21**, 86–89.